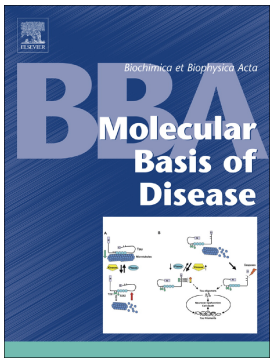
Accepted Manuscript




# Cardiomyocyte-specific knockout of endothelin receptor a attenuates obesity cardiomyopathy

Asli F. Ceylan, Shuyi Wang, Machender R. Kandadi, Jie Chen, Yinan Hua, Zhaohui Pei, Sreejayan Nair, Jun Ren

PII: S0925-4439(18)30263-1
DOI: doi:10.1016/j.bbadis.2018.07.020
Reference: BBADIS 65190

To appear in: *BBA - Molecular Basis of Disease*

Received date: 11 March 2018
Revised date: 14 July 2018
Accepted date: 16 July 2018

Please cite this article as: Asli F. Ceylan, Shuyi Wang, Machender R. Kandadi, Jie Chen, Yinan Hua, Zhaohui Pei, Sreejayan Nair, Jun Ren , Cardiomyocyte-specific knockout of endothelin receptor a attenuates obesity cardiomyopathy. Bbadis (2018), doi:10.1016/j.bbadis.2018.07.020

This is a PDF file of an unedited manuscript that has been accepted for publication. As a service to our customers we are providing this early version of the manuscript. The manuscript will undergo copyediting, typesetting, and review of the resulting proof before it is published in its final form. Please note that during the production process errors may be discovered which could affect the content, and all legal disclaimers that apply to the journal pertain.

ACCEPTED MANUSCRIPT

# Cardiomyocyte-Specific Knockout of Endothelin Receptor A Attenuates Obesity Cardiomyopathy

**Asli F. Ceylan[1,2]*, Shuyi Wang[1*], Machender R. Kandadi[1],[*] Jie Chen[3], Yinan Hua[1], Zhaohui Pei[3], Sreejayan Nair[1] and Jun Ren[1]**

**[1]Center for Cardiovascular Research and Alternative Medicine, University of Wyoming College of Health Sciences, Laramie, WY 82071, USA; [2]Faculty of Medicine, Ankara Yildirim Beyazit University, Ankara, TURKEY; [3]The Second Department of Cardiology, The Third Hospital of Nanchang, Nanchang, Jiangxi 330009, China**

***Equal contribution**

**Running Title:** ETA receptor and obesity cardiomyopathy

**Correspondence should be addressed to:**

**Jun Ren or Sreejayan Nair, University of Wyoming College of Health Sciences, Laramie, WY 82071, USA; Tel: (307)766-6131; Fax: (307)766-2953; E-mail: jren@uwyo.edu or sreejay@uwyo.edu or Zhaohui Pei, The Second Department of Cardiology, The Third Hospital of Nanchang, Nanchang, Jianxi 330009, China; E-mail: leak123@126.com**

ACCEPTED MANUSCRIPT


## ABSTRACT

Endothelin (ET)-1 is implicated in the pathophysiology of cardiovascular diseases although its role in obesity anomalies has not been fully elucidated. This study was designed to examine the impact of ET-1 receptor A ($ET_A$) ablation on obesity-induced changes in cardiac geometry and contractile function, as well as the mechanisms involved with a focus on autophagy. Cardiomyocyte-specific $ET_A$ receptor knockout (ETAKO) and WT mice were fed either low-fat (10% calorie from fat) or high-fat (45% calorie from fat) diet for 24 weeks. Glucose tolerance test was examined to confirm insulin resistance. High-fat diet intake compromised myocardial geometry (enlarged left ventricular diameters in systole and diastole), morphology (cardiac hypertrophy, increased wall thickness and interstitial fibrosis), contractile function (reduced fractional shortening, ejection fraction and cardiomyocyte shortening) and intracellular $Ca^{2+}$ handling, the effect of which was significantly attenuated by ETAKO. TUNEL staining revealed overt apoptosis in high-fat-fed group, the effect was reverted by ETAKO. Western blot analysis noted that high-fat intake downregulated leptin receptor and PPARγ, insulin signaling (elevated basal/dampened insulin-stimulated phosphorylation of Akt and IRS1), phosphorylation of AMPK, ACC, upregulated GATA-4, ANP, NFATc3, PPARα, m-TOR/p70s6k signaling, which were attenuated by ETAKO with the exception of AMPK/ACC. Furthermore, high-fat intake suppressed cardiac autophagy, which was abrogated by ETAKO. In cultured murine cardiomyocytes, palmitic acid challenged mimicked high-fat diet-induced hypertrophic and autophagic responses, the effect of which were abolished by the $ET_A$ receptor antagonist BQ123 or mTOR inhibitor rapamycin. These results suggest that inhibition of $ET_A$ rescues high-fat intake-induced cardiac anomalies possibly through autophagy regulation.


**Key words:** Endothelin-1, obesity, heart, high-fat diet, hypertrophy, contractility, autophagy

ACCEPTED MANUSCRIPT

## 1. INTRODUCTION

Uncorrected obesity has been a major health problem and the prevalence of obesity is fast rising reaching an epidemic proportion [1-3]. Ample of clinical and experimental evidence has suggested that obesity leads to intrinsic changes in the heart including cardiac hypertrophy, an adaptive response initially capable of compensating for the increased myocardial workload, in an effort to maintain normal cardiac function. However, with persistent fat diet intake and adiposity, the physiological cardiac remodeling often develops into maladaptive pathological hypertrophy, resulting in progression of cardiac contractile dysfunction and ultimately heart failure [4-6]. Not surprisingly, obesity is deemed as a major independent risk factor for the ever-rising cardiac morbidity and mortality [6-8].

Endothelin-1 (ET-1) is a potent vasoconstrictor peptide released in vascular endothelium and participates in a wide variety of pathophysiological processes [9]. Aberrant production and activity of ET-1 are considered a hallmark of obesity and related cardiovascular dysfunction [10, 11]. ET-1 exerts its biological effects via the $ET_A$ and $ET_B$ receptors. Although both receptors are ubiquitously expressed, >90% of ET receptors in cardiomyocytes are $ET_A$ subtype [12]. Human and animal studies have indicated elevated plasma and tissue levels of ET-1, and enhanced expression of $ET_A$ receptors in various cardiovascular anomalies [13-16]. Consequently, ET-1 receptor antagonists have displayed beneficial therapeutic effects against ischemia-reperfusion injury, aging, cold stress, endothelial dysfunction, hypertension, cardiovascular remodeling, and heart failure [17-21]. However, little information is available for the role of ET-1 inhibition in obesity-associated cardiac dysfunction. Given the essential role for ET-1 in the pathogenesis and therapeutics in cardiovascular disease in particular obesity complications [10, 11, 20-22], this study was designed to evaluate the impact of knockout of $ET_A$ (ETAKO) on cardiac function in a

ACCEPTED MANUSCRIPT

high-fat diet-induced model of obesity. In an effort to examine the possible mechanism of action involved in ETAKO-offered response against obesity cardiomyopathy, if any, wild-type (WT) and cardiac-specific $ET_A$ knockout mice were fed high-fat or low-fat diet for 6 months prior to the assessment of cardiac geometry, morphology, insulin sensitivity, apoptosis, energy sensing, substrate utilization, and the mitochondrial biogenesis cofactor peroxisome proliferator-activated receptor-γ coactivator-1α (PGC-1α).

## 2. MATERIALS AND METHODS

***2.1: High fat diet feeding and oral glucose tolerance test (OGTT):*** The experimental procedures described in this study were approved by the University of Wyoming Animal Use and Care Committee (Laramie, WY, USA). In brief, weaning 4-week-old male cardiomyocyte-specific endothelin A receptor knockout (ETAKO) mice with a background of C57B1/6xJ29sv (kindly provided by Dr. Masashi Yanagisawa, University of Texas Southwestern Medical Center, Dallas, TX) [23] and age-/gender-matched littermates (served as WT) were randomly assigned to low-fat (10% kcal % fat; Research Diets, New Brunswick, NJ; #D12450B) or high-fat diet (45% kcal % fat; NJ; #D12451) [24]. Following the 6-month feeding, mice were fasted for 12 hrs and were given glucose (2 g/kg body weight) using gavage. Blood samples were drawn from tails immediately before the glucose challenge and 30, 60 and 120 min thereafter using an Accu-Chek III glucose analyzer [25]. Following the completion of OGTT, mice were placed on with respective diet *ad libitum* for 2 more days prior to experimentation or sacrifice for tissue collection.

ACCEPTED MANUSCRIPT

**2.2:** ***Echocardiographic assessment:*** Cardiac geometry and function were evaluated in anesthetized (ketamine 80 mg/kg and xylazine 12 mg/kg, i.p.) mice using a 2-dimensional guided M-mode echocardiography (Phillips Sonos 5500) equipped with a 15-6 MHz linear transducer (Phillips Medical Systems, Andover, MD). Anterior and posterior wall thickness and diastolic and systolic left ventricular dimensions were recorded from M-mode images using the method adopted by the American Society of Echocardiography. Fractional shortening was calculated from end-diastolic diameter (EDD) and end-systolic diameter (ESD) using the equation: (EDD-ESD)/EDD. Left ventricular (LV) mass was calculated from LVIDd (LV internal dimension at end-diastole), LVPWd (left ventricular posterior wall diameter) and IVSd (interventricular septal thickness) using the equation, LV mass = 1.055 x [(LVPWD + LVIDD + IVSD)$^3$-LVIDD$^3$] x 1000. Heart rates were averaged over 10 cardiac cycles [25].

***2.3: Blood pressure measurement and cardiac triglyceride levels:*** Systolic and diastolic blood pressure were measured using a CODA semi-automated non-invasive blood pressure device (Kent Scientific Co, Torrington, CT). Cardiac triglyceride level was measured by a colorimetric kit from Biovision (Mountain View, CA). Heart samples were homogenized and heated in 5% NP-40 solution to 90°C for 5 min to solubilize triglyceride before the lysate was centrifuged for 2 min. The supernatant was used for triglyceride assay per the manufactures instructions [26].

***2.4: Histopathological analysis and TUNEL staining:*** Ventricular tissues were stained with FITC-conjugated wheat germ agglutinin and cardiomyocyte cross-sectional area was quantitated by measuring 60 random cardiomyocytes per microscopic field. Masson trichrome and TUNEL staining were employed to assess interstitial fibrosis and apoptosis, respectively. Percentage of

ACCEPTED MANUSCRIPT

fibrosis was calculated using the histogram function of the photoshop software [24]. Apoptotic cardiomyocytes were monitored using the In Situ Death Detection Kit (Roche, Branchburg, NJ) and TUNEL positive cells were normalized to total cell number [27].

***2.5: Cardiomyocyte isolation and drug treatment:*** After ketamine/xylazine sedation, hearts were removed and perfused with Krebs-Henseleit bicarbonate (KHB) buffer containing (in mM): 118 NaCl, 4.7 KCl, 1.2 $MgSO_4$, 1.2 $KH_2PO_4$, 25 $NaHCO_3$, 10 HEPES, and 11.1 glucose. Hearts were digested with collagenase D for 20 min. Left ventricles were removed and minced before being filtered. Cardiomyocyte yield was ~75%. Only rod-shaped myocytes with clear edges were selected for mechanical and intracellular $Ca^{2+}$ studies. To evaluate the role of $ET_A$ receptor and mTOR in high fat diet intake-induced changes in autophagic and hypertrophic response, a cohort of cardiomyocytes from WT mice were treated with palmitic acid (0.5 mM) for 6 hrs [24] in the presence and absence of the $ET_A$-receptor antagonist BQ123 (5 µM) [28] or the mTOR inhibitor rapamycin (5 µM) [29] prior to assessment of hypertrophy and autophagy markers.

***2.6: Cell shortening/relengthening:*** Mechanical properties of cardiomyocytes were assessed using an IonOptix soft-edge system (IonOptix, Milton, MA). Myocytes were placed in a chamber mounted on the stage of an Olympus IX-70 microscope and superfused (~2 ml/min at 25°C) with a Krebs-Henseleit bicarbonate buffer containing 1 mM $CaCl_2$. Myocytes were field stimulated at 0.5 Hz unless otherwise stated. Cell shortening and relengthening were assessed including peak shortening, indicating peak contractility; time-to-PS (TPS), indicating contraction duration; time-to-90% relengthening ($TR_{90}$), indicating relaxation duration; and maximal

ACCEPTED MANUSCRIPT

velocities of shortening/relengthening (± dL/dt), indicating maximal pressure development and decline [24].

***2.7: Intracellular $Ca^{2+}$ transients:*** A cohort of myocytes was loaded with fura-2/AM (0.5 μM) for 10 min, and fluorescence intensity was recorded with a dual-excitation fluorescence photomultiplier system (IonOptix®). Myocytes were placed onto an Olympus IX-70 inverted microscope and imaged through a Fluor 40X-oil objective. Cells were exposed to light emitted by a 75W mercury lamp and passed through either a 360- or a 380-nm filter, while being stimulated to contract at 0.5 Hz. Fluorescence emissions were detected between 480 nm and 520 nm, and qualitative changes in fura-2 fluorescence intensity (FFI) was inferred from FFI ratio at two wavelengths (360/389). Intracellular $Ca^{2+}$ decay was presented either in curve fitting-generated decay rate or area underneath the intracellular $Ca^{2+}$ transient curve [24].

***2.8: Western blot analysis:*** Left ventricular tissues or isolated cardiomyocytes from mice were homogenized and centrifuged at 70,000 x *g* for 20 min at 4°C. The supernatants were used for immunoblotting. The extracted proteins were separated on 10-15% SDS-polyacrylamide gel and were transferred to nitrocellulose membranes. Following the block, the membrane was incubated with anti-$ET_A$ receptor, anti-$ET_B$ receptor, anti-Ob-R (leptin receptor), anti-protein tyrosine phosphate 1B (PTP1B), anti-sarco(endo)plasmic reticulum $Ca^{2+}$-ATPase 2a (SERCA2a), anti-$Na^{+}$-$Ca^{2+}$ exchanger, anti-phospholamban, anti-Akt, anti-phospho-Akt ($Thr^{308}$), anti-insulin receptor substrate 1 (IRS1), anti-phospho-IRS1 ($Tyr^{941}$), anti-GATA4, anti-ANP, anti-nuclear factor of activated T cells (NFATc3), anti-PPARα, anti-PPARγ, anti-PGC1α, anti-pyruvate dehydrogenase (PDH), anti-phospho-PDH ($Ser^{291}$), anti-AMPK, anti-phospho-AMPK ($Thr^{172}$),

ACCEPTED MANUSCRIPT

anti-ACC, anti-phospho-ACC ($Ser^{79}$), anti-malonly Co-A decarboxylase (MCD), anti-Beclin1, anti-LC3B, anti-Atg7, anti-Atg12, anti-mTOR, anti-phospho-mTOR ($Ser^{2448}$), anti-p70s6k, anti-phospho-p70s6k ($Thr^{389}$) and anti-GAPDH antibodies. All antibodies were used at a dilution factor of 1:1,000 at 4°C overnight. After incubation with the primary antibodies, blots were incubated with horseradish peroxidase-linked secondary antibodies (1:5,000) for 60min at room temperature. Immunoreactive bands were detected using the Super Signal West Dura Extended Duration Substrate (Pierce, Milwaukee, WI). The intensity of bands was measured with a scanning densitometer (Model GS-800; Bio-Rad) coupled with a Bio-Rad personal computer analysis software [24].

***2.9: Assessment of mRNA expression by quantitative real-time PCR:*** Total RNA was isolated from left ventricles followed by DNase digestion to eliminate genomic DNA contamination. Synthesis of cDNA was performed at $37^0$C for 60min using 1 µg total RNA in a 20µL system by Superscript III (Invitrogen). Quantitative real-time reverse-transcription PCR (qRT-PCR) analysis was performed for β-myosin heavy chain (β-MHC), atrial natriuretic peptide (ANP), and brain natriuretic peptide (BNP) using appropriate primers. Results are expressed relative to GAPDH using $\Delta C_T$ method [29]. The sequences of primers are listed in Table 1.

***2.10: Statistical analysis:*** Data were mean ± SEM. Normality distribution of data was checked using D'Agostino-Pearson omnibus normality test of GraphPad Prism (version 6.0, $p > 0.05$ for a pass). Statistical significance ($p < 0.05$) for each variable was determined by a one-way ANOVA (two-way for OGTT) followed by Tukey's post hoc test.

ACCEPTED MANUSCRIPT

## 3. RESULTS

### 3.1: General features and echocardiographic properties

OGTT revealed that chronic high-fat diet intake impaired glucose disposal as evidenced by delayed glucose clearance after peaking of blood glucose levels with oral glucose challenge. Mice receiving high-fat diet displayed significantly higher blood glucose levels following OGTT and maintained higher glucose levels compared with mice fed low-fat diet. ETAKO did not affect glucose handling in either diet group, indicating that cardiomyocyte-specific ETAKO does not alter obesity-associated impairment in glucose disposal (Supplemental Fig. 1). As shown in Table 2, high-fat diet intake overtly increased body weights in a comparable manner in both WT and ETAKO mice. High fat diet intake significantly increased heart, liver and kidney weights. Although ETAKO itself exhibited little effect on body and organ weights under low-fat diet intake, it overtly attenuated high-fat diet intake-induced increase in heart but not liver and kidney weights (or changes in organ size). In addition, echocardiographic evaluation revealed that high-fat diet increased diastolic diameter (EDD), systolic diameter (ESD) and left ventricular (LV) wall thickness as well as LV mass, all of which were significantly attenuated or mitigated by ETAKO. Furthermore, chronic high fat diet intake elicited overt reduction in both fractional shortening and ejection fraction, the effects of which were nullified by ETAKO. Heart rate was comparable among all experimental groups. Systolic but not diastolic blood pressure was elevated following high-fat intake, the effect of which was unaffected by ETAKO. ETAKO itself did not affect systolic or diastolic blood pressure under normal diet regimen as well. Assessment of cardiac triglyceride levels revealed that chronic high fat diet intake significantly increased the cardiac triglyceride levels, the effect of which was significantly attenuated by ETAKO.

ACCEPTED MANUSCRIPT

### 3.2: Mechanical and intracellular $Ca^{2+}$ properties of cardiomyocytes

High-fat-induced obesity overtly increased resting cardiomyocyte cell length, decreased peak shortening, maximal velocity of shortening and relengthening as well as prolonged TPS and $TR_{90}$ in cardiomyocytes. Although ETAKO itself did not exert any notable effect on mechanical properties in cardiomyocytes, it ablated high fat diet-induced alterations in cardiomyocyte cell length and contractile anomalies (Fig. 1A-F). Furthermore, diet-induced obesity significantly elevated baseline intracellular $Ca^{2+}$ (FFI), suppressed electrically-stimulated intracellular $Ca^{2+}$ rise (ΔFFI), and prolonged intracellular $Ca^{2+}$ decay, all of which was reconciled by ETAKO. In contrast, ETAKO itself did not alter intracellular $Ca^{2+}$ properties in low-fat fed mice (Fig. 1G-I).

### 3.3: Effect of ETAKO on cardiac remodeling and apoptosis in diet-induced obesity

High-fat diet-induced obesity elicited a significant rise in the cardiomyocyte transverse cross-sectional area, consistent with the increased heart weight and LV mass (Fig. 2A and Fig. 2C). The cardiomyocyte hypertrophy in diet-induced obesity was negated by ETAKO. Likewise, an increase in interstitial fibrosis (assessed using Masson's trichome staining) was evident in the hearts from high-fat-fed WT mice but not in high-fat-fed ETAKO mice (Fig. 2B and Fig. 2D). ETAKO itself did not exert any notable effect on cardiac remodeling in the low-fat-fed mice. In addition, high-fat diet-induced obesity led to a significant increase of cardiomyocyte apoptosis as assessed using TUNEL staining, the effect of which was ablated by ETAKO. ETAKO itself failed to affect the levels of apoptosis in low-fat diet-fed mice (Fig. 3).

### 3.4: Effect of ETAKO on cardiac ET receptors, hypertrophic protein and mRNA

ACCEPTED MANUSCRIPT

High-fat diet-induced obesity led to upregulation of $ET_A$ receptor without affecting $ET_B$ receptor. ETAKO ablated $ET_A$ receptor without affecting levels of $ET_B$ receptor, under either diet regimen (Fig. 4D-F). Diet-induced obesity significantly increased mRNA levels of β-myosin heavy chain (β-MHC), BNP and ANP, the effect of which was reconciled by ETAKO. ETAKO itself did not affect the mRNA levels of these pro-hypertrophic markers (Fig. 4A-C). Consistent with the mRNA result, diet-induced obesity significantly upregulated protein levels of GATA4, ANP and NFATc3. ETAKO itself did not affect protein levels of these pro-hypertrophic markers although it nullified high-fat diet-induced upregulation of hypertrophic proteins (Fig. 4D, G-I).

### 3.5: Effect of ETAKO on insulin signaling and intracellular $Ca^{2+}$ regulatory proteins in fat diet-induced obesity

Obesity is commonly associated with altered leptin signaling mainly manifested as leptin resistance [30]. Our data revealed that diet-induced obesity significantly downregulated Ob-R leptin receptor and upregulated the negative regulator of insulin signaling PTP1B, the effect of which was unaffected by ETAKO. Prolonged high-fat diet intake also overtly downregulated the intracellular $Ca^{2+}$ regulatory proteins SERCA2a and $Na^+$-$Ca^{2+}$ exchanger and upregulated levels of phospholamban, an inhibitory regulator of SERCA2a, the effect of which was significantly attenuated or reversed by ETAKO. ETAKO itself did not affect the levels of Ob-R, PTP1B, SERCA2a, $Na^+$-$Ca^{2+}$ exchanger and phospholamban (Fig. 5A-F). To further discern insulin sensitivity, a cohort of low- or high-fat-fed mice were challenged with insulin (5 mU/g body weight, i.p.) for 10 min [31] prior to tissue collection. Our data shown in Fig. 5G-I showed that high-fat diet intake significantly increased the basal phosphorylation of Akt and IRS1 (tyrosine) although it dampened insulin-stimulated phosphorylation of Akt and IRS1. Although ETAKO

ACCEPTED MANUSCRIPT

itself did not affect basal or insulin-stimulated phosphorylation of Akt and IRS1, it negated high-fat diet-induced changes in both basal and insulin-stimulated phosphorylation of Akt and IRS1.

### 3.6: Effect of ETAKO on energy sensing and substrate utilization in diet-induced obesity

Obesity is accompanied with a shift in both energy sensing and substrate utilization (in favor of fatty acids) [32]. To evaluate the role of energy sensing and substrate utilization in ETAKO- and high-fat diet-induced cardiac responses, levels of peroxisome proliferator-activated receptor-α and -γ (PPARα and PPARγ), nuclear receptors governing transcriptional regulation of lipid metabolism and energy balance [33], acetyl-CoA carboxylase (ACC) which synthesizes the key metabolic effector for obesity and cardiac fatty acid oxidation, malonyl Co-A, and malonyl-CoA decarboxylase (MCD), which degrades malonyl Co-A [34], were evaluated. ACC upstream metabolic and cellular fuel sensor AMPK and phosphorylation of pyruvate dehydrogenase (PDH), essential substrate for cardiac energy metabolism [35], were also monitored. High-fat diet intake significantly upregulated PPARα, downregulated PPARγ, mitochondrial biogenesis cofactor PGC1α, and MCD, and suppressed phosphorylation of PDH, AMPK and ACC. Although ETAKO itself did not affect the levels of these energy sensing and substrate utilization proteins, it partially attenuated or nullified high-fat diet -induced changes in PPARα, PPARγ, and PGC1α without affecting MCD and phosphorylation of PDH, AMPK and ACC (Fig. 6). These data favor that ETAKO might not overtly affect energy sensing and substrate utilization (albeit with improved lipid metabolism and mitochondrial content) in diet-induced obesity.

### 3.7: Effect of ETAKO on myocardial autophagy in diet-induced obesity

ACCEPTED MANUSCRIPT

Obesity is commonly associated with compromised autophagy clearance mechanism [2]. Our data shown in Fig. 7 depicted that diet-induced obesity significantly suppressed autophagy including Atg7, Atg12 and LCBII/I ratio and elevated p62 without changes in Beclin1. ETAKO itself did not exert any notable effect on autophagy although it effectively restored high-fat diet-induced changes in these autophagy protein markers. Neither ETAKO nor high-fat diet intake overtly affected the levels of LC3BI. These data indicate that ETAKO reverses high-fat diet-induced suppression of autophagy.

### 3.8: Effect of ETAKO on myocardial mTOR signaling in high fat diet-induced obesity

In cardiac hypertrophy, mTOR is activated by the PI3-kinase/Akt-pathway, which in turn regulates cell size via the rapamycin-sensitive adaptor protein of mTOR (Raptor) and rapamycin-insensitive companion of mTOR (Rictor), as well as subsequent complex activation [36]. High-fat diet significantly promoted phosphorylation of mTOR and its downstream signaling molecule p70s6k, as well as upregulated Raptor and Rictor, the effect of which was reversed by ETAKO with little effect from ETAKO itself in the face of low-fat diet intake (Fig. 8). These data indicate a role for mTOR signaling in high-fat diet- and ETAKO-induced cardiac mechanical, hypertrophic and autophagy (considering the role of mTOR as the most fundamental autophagy inhibitor) responses.

### 3.9: Effect of inhibition of $ET_A$ receptor and mTOR on palmitic acid-induced hypertrophic and autophagic responses in murine cardiomyocytes

To ascertain the role of $ET_A$ and mTOR in obesity-induced cardiomyocyte hypertrophic and autophagic responses, murine cardiomyocytes from WT mice were challenged with palmitic

ACCEPTED MANUSCRIPT

acid (0.5 mM for 6 hrs) [24] to mimic the obesogenic environment *in vivo* in the presence or absence of BQ123, a pharmacological antagonist of the $ET_A$ receptor, or rapamycin, an inhibitor of mTOR. As shown in Fig. 9, palmitic acid challenge *in vitro* resulted in a downregulation of autophagy protein markers (Atg7, Atg12, LC3BII-to-LC3BI ratio but not Beclin1), elevated phosphorylation of mTOR as well as upregulation of hypertrophic protein markers GATA4, ANP and NFATc3, the effects of which were abolished by BQ123 and rapamycin. Neither BQ123 nor rapamycin overtly affected the protein levels of these autophagic and hypertrophic protein markers.

## 4. DISCUSSION

Aberrant production and activity of ET-1 are considered hallmarks in obesity [10, 11]. Ample of evidence has documented a detrimental pathological role of ET-1 in the development of heart diseases [37-39]. Consequently, inhibition of $ET_A$ may serve as a potential strategy in the management of cardiovascular and metabolic diseases. The salient findings from our current study revealed that cardiomyocyte-specific knockout of $ET_A$ receptors attenuated high-fat diet-induced cardiac remodeling, contractile dysfunction, apoptosis, and autophagy failure. These fat diet-induced obesity-associated alterations in cardiac geometry and contractile function were accompanied with elevated cardiac triglycerides, upregulation of hypertrophic genes/proteins (β-MHC, ANF, GATA4 and NFATc3), compromised insulin signaling, activation of the mTOR-signaling and downregulation of autophagy, which were reconciled by ETAKO. Consistent with these in vivo data, in vitro challenge of palmitic acid to mimic obesogenic environment yielded reminiscent changes in pro-hypertrophic and autophagic signaling in murine cardiomyocytes. Interestingly, inhibition of $ET_A$ receptor using a pharmacological inhibitor or induction of

ACCEPTED MANUSCRIPT

autophagy (inhibition of mTOR) using rapamycin effectively reversed palmitic acid-induced changes in the aforementioned cellular signaling. Taken together, these results favor the notion that ablation of $ET_A$ mitigates high-fat diet-induced deleterious effects on cardiac hypertrophy and contractile dysfunction via down-regulation of mTOR and stimulation of autophagy.

Ample evidence has shown that ET-1 system plays a pivotal role in the development of cardiovascular anomalies and pharmacological inhibition of $ET_A$ prevents the development of cardiac hypertrophy [37-39]. Yanagisawa and coworkers, who first reported the cardiomyocyte-specific endothelin A receptor knockout mice, failed to note any protective effect of ETAKO on angiotensin II or isoproterenol induced cardiac hypertrophic or contractile response [23]. Evidence from our group using the same murine model revealed beneficial effect of ETAKO against aging and cold stress-induced cardiac pathological changes [20, 21]. One plausible reason for this discrepancy may be the compensatory upregulation of $ET_B$ receptor [23]. It is also likely that angiotensin II and isoproterenol may be mediating their hypertrophic effects in an endothelin-independent manner. However, our study did not favor compensatory upregulation of $ET_B$ receptor in the face of high-fat diet intake. ET-1 and isoproterenol were shown to induce cardiac hypertrophy through distinct signaling mechanisms [40]. While ET-1 phosphorylates glycogen synthase kinase-3β (GSK3β) through the mitogen-activated protein kinase (MAPK) and phosphatidylinositol-3-kinase (PI3K)/Akt cascades, isoproterenol activates GSK3β primarily via PI3K/Akt signaling. Although the precise mechanisms involved in obesity-associated cardiac hypertrophy and contractile dysfunction remain elusive, it is likely that certain pathways other than neurohormonal signaling may be involved in the observed beneficial effects of ETAKO.

Sustained obesity leads to dyslipidemia, glucose intolerance, insulin resistance, leptin resistance and inflammation, all of which may predispose devastating cardiac complications such

ACCEPTED MANUSCRIPT

as cardiac hypertrophy and heart failure [1-3, 41]. This is supported by elevated cardiac triglycerides, downregulated Ob-R, and compromised insulin signaling (OGTT, phosphorylation of Akt and IRS1, as well as upregulated PTP1B) observed in our study. Although one may argue that high-fat diet per se may predispose cardiac remodeling and contractile dysfunction, findings from our group previously suggested that it is the diet-induced obesity rather than high fat diet itself that promotes cardiac remodeling and contractile dysfunction [42]. At the cellular level, development of cardiac hypertrophy in diet-induced obesity (heart weight, LV mass, and cross-sectional area) involves signaling pathways leading to alterations in gene transcription and protein synthesis such as β-MHC, ANF, GATA4 and NFATc3 as observed in our current study. Calcineurin-mediated dephosphorylation of NFATc leads to its nuclear translocation to interact with cardiac–restricted zinc finger protein GATA-4, en route to the upregulation of hypertrophic genes [43]. In this study, we found that ETAKO attenuated high-fat diet-mediated upregulation of hypertrophic genes and proteins, consistent with its response on cardiac hypertrophy. Ehmke and co-workers found similar rises in hypertrophic proteins associated with renal artery clipping in mice, the effect of which was inhibited by a pharmacological $ET_A$ receptor antagonist [44]. These authors did not observe any changes in blood pressure following $ET_A$ receptor blockade, suggesting a cardiomyocyte-specific effect. This is also consistent with our observations, where ETAKO failed to alter global parameters such as body (and liver/kidney) weight, blood pressure and glucose handling. Furthermore, our in vitro finding that exogenous palmitic acid challenge triggered upregulation of pro-hypertrophic proteins in cardiomyocytes, which was abolished by the $ET_A$ receptor blocker BQ123. In conjunction with the elevated $ET_A$ receptor levels in fat diet-induced obesity, our findings have substantiated the notion of ET-1 in the onset and development

ACCEPTED MANUSCRIPT

of cardiac hypertrophy in obesity. It is noteworthy that leptin signaling and PTP1B were unlikely involved in ETAKO-elicited beneficial cardiac geometric and functional responses.

Our study revealed elevated basal Akt phosphorylation in diet-induced obesity, the effect of which was reversed by ETAKO. Activation of Akt promotes cardiac hypertrophy via a number of cellular mechanisms including activation of its downstream targets such as mTOR and GSK3β [45, 46]. Short-term activation of Akt stimulates physiological hypertrophy and is thought to be cardio-protective. On the other side of the coin, chronic activation of Akt leads to pathological hypertrophy and eventually heart failure [47-50]. The presence of contractile dysfunction, interstitial fibrosis, apoptosis and re-expression of fetal cardiac genes (e.g., ANP and β-MHC) are strong indicative of presence of pathological hypertrophy in our high-fat diet-induced obesity model. Consequently, activation of Akt (basal phosphorylation) in chronic high-fat diet fed mice should represent a detrimental event and inhibition of Akt activation with $ET_A$ knockout may therefore be protective.

mTOR is linked to nutrient sensing and protein synthesis in the heart, and is involved in cardiomyocyte hypertrophy [51]. Our current study showed that high-fat diet intake (or palmitic acid) turned on Akt/mTOR pro-hypertrophic signaling, the effect of which was abrogated by $ET_A$ receptor knockout (in vivo) or BQ123 (in vitro). Previous studies by Wang and coworkers showed that ET-1 inhibited ribosomal S6 kinase (p70s6k), a downstream effector of mTOR [52], which is consistent with our current observation. In addition, rapamycin, an inhibitor of mTOR (and an inducer of autophagy), reversed palmitic acid-mediated hypertrophic responses in murine cardiomyocytes. While the interaction of mTOR with Rictor stimulates cell growth and protein synthesis via phosphorylation of p70s6k, the Rictor complex is implicated in cytoskeletal rearrangement and cell survival [53]. Our data of restored levels of Raptor and Rictor in ETAKO

ACCEPTED MANUSCRIPT

mice fed high-fat diet suggest that possible involvement of both mTOR-dependent and –independent mechanisms in $ET_A$ receptor knockout-offered beneficial response against high-fat diet intake. Taken together, it is plausible that ET-1/$ET_A$ signaling mediates cardiac hypertrophy by upregulating the Akt/mTOR signaling as depicted in Fig. 10.

Our results indicated that ETAKO effectively restored compromised autophagy in diet-induced obesity. Autophagy is a conserved cellular process through which cytoplasmic contents including proteins and organelles are degraded in lysosomes [54]. Autophagy maintains cellular homeostasis in the heart and serves as a 'double-edged sword' for both metabolic and cardiac homeostasis [2, 55, 56]. Both suppressed and over-activated autophagy have been documented in obesity and other metabolic anomalies [2]. In the realm of obesity, it is generally perceived that autophagy is upregulated in adipose tissues, while it is mostly downregulated in the liver, heart and pancreas [2, 57]. Recent evidence has demonstrated suppressed autophagy in diet-induced and genetically-predispose obese hearts [2, 58, 59], similar to our current study. However, contrary finding of elevated autophagy was also noted in high-fat diet-induced obese hearts [60]. These findings suggest the complex nature of autophagy regulation in obesity possibly due to experimental models and duration of adiposity. The Akt/mTOR signaling cascade negatively regulates autophagy [61] whereas rapamycin induces autophagy through inhibiting mTOR. Last but not least, the ETAKO-induced restoration of autophagy may contribute to the improved lipid metabolism noted in our study (cardiac triglycerides, PPARα, PPARγ and PGC1α) as depicted in Fig. 10. Although ETAKO is unlikely to improve cardiac homeostasis through correcting obesity-induced changes in energy sensing and substrate utilization (AMPK-ACC- or MCD-mediated malonyl Co-A production or degradation, or cardiac energy metabolism through PDH

ACCEPTED MANUSCRIPT

phosphorylation), improved autophagy should help to clear lipid deposit from the obese hearts as suggested by "lipophagy" [2].

Experimental limitations: Although our data suggest that ETAKO may rescue against diet-induced obesity-related cardiac anomalies through rescuing autophagy, several experimental limitations must be considered. First, possible involvement of neurohormonal system should not be discounted as $ET_A$ inhibition may decrease circulating catecholamine levels, thus benefiting cardiac geometry and function indirectly. Second, further study is needed to elaborate the precise role of mitochondrial function as little is known with regards to how restored autophagy corrects PGC1α levels and apoptosis. Last but not least, more discrete measurement of autophagy such as using GFP-puncta (although there was technical difficulty of evaluating GFP-puncta in murine cardiomyocytes in our current study) would help to get a better assessment of autophagy.

In summary, our data show that cardiomyocyte-specific knockout of $ET_A$ receptor protects against diet-induced obesity-associated cardiac hypertrophy and contractile dysfunction. The anti-hypertrophic effects of $ET_A$ knockout may be attributable to inhibition of the IRS1-Akt-mTOR mediated pro-hypertrophic signaling cascade, which would restore autophagy in obesity (Fig. 10). Taken together, these findings support the growing body of evidence suggesting the therapeutic utility of targeting ET-1 in the management of obesity-associated cardiovascular complications. Cardiac hypertrophy is prevalent in obese individuals and is an independent risk factor for cardiovascular disease [1, 3, 41]. However, left ventricular hypertrophy may also serve as a useful adaptation for ventricles to cope with chronic stress or overload. Better prognosis of cardiovascular complication has been indicated in obese subjects compared to lean subjects, a clinical phenomenon commonly referred to as 'obesity paradox' [5, 62]. Nonetheless, given that the current evidence supports the unfavorable effects of overweight/obesity in the development

ACCEPTED MANUSCRIPT

of cardiovascular disease [2], it may be prudent to consider $ET_A$ receptor antagonists as potential interventional strategies in the management of obesity-associated cardiovascular diseases.

ACCEPTED MANUSCRIPT

ACCEPTED MANUSCRIPT

## 5. ACKNOWLEDGMENTS

The $ET_A$ knockout mice were kindly provided by Professor Masashi Yanagisawa from Howard Hughes Medical Institute, University of Texas Southwestern Medical Center, Dallas, TX 75390, USA.

## 6. SOURCES OF FUNDING

This work was supported in part by NIH/NCRR P20 RR016474.

## 7. DISCLOSURES

None of the authors have any competing conflict of interest to declare.

ACCEPTED MANUSCRIPT

ACCEPTED MANUSCRIPT

## 8. FIGURE LEGENDS

Fig. 1 Cardiomyocyte contractile and intracellular $Ca^{2+}$ properties in WT and ETAKO mice fed either low-fat (LF, 10%) or high-fat (HF, 45%) diet for 6 months. A: Resting cell length; B: Peak shortening (PS); C: Maximal velocity of shortening (+ dL/dt); D: Maximal velocity of relengthening (- dL/dt); E: Time-to-PS (TPS); F: Time-to-90% relengthening ($TR_{90}$); G: Resting fura-2 fluorescence intensity (FFI); H: Change of intracellular $Ca^{2+}$ in response to electrical stimuli (ΔFFI); and I: Intracellular $Ca^{2+}$ decay rate. Mean ± SEM, n = 65 - 78 cells from 4 mice per group for panels A-F; n = 45 - 49 cells from 3 mice per group for panels G-I, *p < 0.05 *vs.* WT-LF, # p < 0.05 *vs.* WT-HF group.

Fig. 2: Histological analysis of myocardial morphology in WT and ETAKO mice fed either low-fat (LF, 10%) or high-fat (HF, 45%) diet for 6 months. A: Representative FITC-conjugated lectin staining depicting transverse sections of left ventricular myocardium (×400); B: Representative Masson Trichrome staining depicting interstitial fibrosis of left ventricular myocardium (×200); C: Quantitative analysis of cardiomyocyte cross-sectional area; and D: Quantitative analysis of interstitial fibrotic area. Mean ± SEM, n = 8 - 12 fields from three mice per group, *p < 0.05 *vs.* WT-LF, # p < 0.05 *vs.* WT-HF group.

Fig. 3: TUNEL apoptosis analysis of hearts from WT and ETAKO mice fed either low-fat (LF, 10%) or high-fat (HF, 45%) diet for 6 months. A: Representative images depicting TUNEL-positive nuclei as visualized with fluorescein (green) in myocardium (×400) from respective mouse groups; and B: Quantitative analysis of TUNEL-positive cells (% of total cell number).

ACCEPTED MANUSCRIPT

Mean ± SEM, n= 17 - 18 fields from three mice per group, *p < 0.05 *vs.* WT-LF, #p < 0.05 *vs.* WT-HF group.

Fig. 4: Hypertrophic gene or protein expression as well as ET receptor levels in hearts from WT and ETAKO mice fed either low-fat (LF, 10%) or high-fat (HF, 45%) diet for 6 months. A: Cardiac β-MHC mRNA levels; B: Cardiac ANP mRNA levels; C: Cardiac BNP mRNA levels; D: Representative gel blots depicting protein levels of $ET_A$ receptor, $ET_B$ receptor, GATA4, ANP and NFATc3 (GAPDH as loading control); E: $ET_A$ receptor; F: $ET_B$ receptor; G: GATA4; H: ANP; and I: NFATc3. Mean ± SEM, n = 5 – 6 hearts per group, *p < 0.05 *vs.* WT-LF, #p < 0.05 *vs.* WT-HF group.

Fig. 5: Insulin signaling and intracellular $Ca^{2+}$ regulatory protein levels in hearts from WT and ETAKO mice fed either low-fat (LF, 10%) or high-fat (HF, 45%) diet for 6 months. A: Representative gel blots depicting protein levels of leptin receptor (Ob-R), PTP1B, SERCA2a, $Na^{+}$-$Ca^{2+}$ exchanger (NCX) and phospholamban (using GAPDH as loading control); B: Ob-R; C: PTP1B; D: SERCA2a; E: NCX; F: Phospholamban; G: Representative gel blots depicting levels of pan and phosphorylated Akt and IRS1 (GAPDH as loading control) in the absence or presence of insulin stimulation (5 mU/g body weight, for 10 min); H: Pan and phosphorylated Akt; and I: Pan and phosphorylated IRS1 (tyrosine). Mean ± SEM, n = 6 – 8 hearts per group, *p < 0.05 *vs.* WT-LF, #p < 0.05 *vs.* WT-HF group, † p < 0.05 *vs.* corresponding insulin unstimulated group.

Fig. 6: Levels of energy sensing molecules PPARα, PPARγ, PGC1α, malonyl-coenzyme A decarboxylase (MCD) as well as phosphorylation of pyruvate dehydrogenase (PDH), AMPK and

ACCEPTED MANUSCRIPT

ACC in hearts from WT and ETAKO mice fed either low-fat (LF, 10%) or high-fat (HF, 45%) diet for 6 months. A: Representative gel blots depicting protein levels of PPARα, PPARγ, PGC1α, MCD, as well as pan and phosphorylated PDH, AMPK and ACC (using GAPDH as loading control); B: PPARα; C: PPARγ; D: PGC1α; E: Phosphorylation of PDH; F: Phosphorylation of AMPK; G: Phosphorylation of ACC; and I: MCD. Mean ± SEM, n = 6 – 8 hearts per group, *p < 0.05 *vs.* WT-LF, #p < 0.05 *vs.* WT-HF group.

Fig. 7: Levels of autophagy markers Beclin1, Atg7, Atg12, LC3B and p62 in hearts from WT and ETAKO mice fed either low-fat (LF, 10%) or high-fat (HF, 45%) diet for 6 months. A: Representative gel blots depicting protein levels of Belcin1, Atg7, Atg12, LC3B, and p62 (using GAPDH as loading control); B: Beclin1; C: Atg7; D: Atg12; E: LC3BII-to-LC3BI ratio; and F: p62. Mean ± SEM, n = 6 hearts per group, *p < 0.05 *vs.* WT-LF, #p < 0.05 *vs.* WT-HF group.

Fig. 8: Levels of proteins involved in autophagy regulation in hearts from WT and ETAKO mice fed either low-fat (LF, 10%) or high-fat (HF, 45%) diet for 6 months. A. Phosphorylation of mTOR; B: Phosphorylation of p70s6k; C: Raptor; and D: Rictor. Insets: Representative gel blots depicting expression of mTOR (pan and phosphorylated), p70s6k (pan and phosphorylated), Raptor, Rictor and GAPDH (loading control) using specific antibodies. Mean ± SEM, n = 5 – 6 hearts per group, *p < 0.05 *vs.* WT-LF, #p < 0.05 *vs.* WT-HF group.

Fig. 9: Changes of autophagy and hypertrophic signaling in mouse cardiomyocytes challenged with palmitic acid (PA, 0.5 mM) for 6 hrs in the presence and absence of the $ET_A$ receptor antagonist BQ123 (5 μM) or the mTOR inhibitor rapamycin (RAPA, 10 μM). A: Representative

ACCEPTED MANUSCRIPT

gel blots depicting levels of Beclin1, Atg7, Atg12, LC3B, mTOR phosphorylation, GATA4, ANP and NFATc3 (using GAPDH as the loading control) using specific antibodies; B: Beclin1; C: Atg7; D: Atg12; E: LC3BII-to-LC3BI ratio; F: phospho-mTOR-to-mTOR ratio; G: GATA4; H: ANP; and I: NFATc3. Mean ± SEM, n = 5 – 7 isolations per group, *p < 0.05 vs. Control, #p < 0.05 *vs.* PA group.

Fig. 10: Schematic diagram depicting the possible roles of $ET_A$ receptor, IRS1, Akt and mTOR signaling in the regulation of autophagy, mitochondrial integrity, cardiac geometry and function in high-fat diet-induced obesity. High-fat diet intake may upregulate ETA receptor, leading to increased basal phosphorylation of IRS1 and Akt (albeit with dampened insulin-stimulated phosphorylation of IRS1 and Akt). In consequence, mTOR phosphorylation is elevated to favor cardiac hypertrophy and suppressed autophagy. High-fat diet intake may also inhibit AMPK-ACC energy sensing and substrate utilization (through malonyl Co-A), the direct effect of which may not be affected by ETAKO. However, improved autophagy in the face of ETAKO may help to improve lipid metabolism to benefit cardiac homeostasis. Arrowheads denote stimulation and the T-end lines represent inhibition. ET-1: endothelin-1; IRS1: insulin receptor substrate 1; MCD: malonyl Co-A decarboxylase; AMPK: AMP-dependent protein kinase; ACC: acetyl-CoA carboxylase.

ACCEPTED MANUSCRIPT

ACCEPTED MANUSCRIPT

## 9. REFERENCES

[1] P. Poirier, T.D. Giles, G.A. Bray, Y. Hong, J.S. Stern, F.X. Pi-Sunyer, R.H. Eckel, A. American Heart, P.A. Obesity Committee of the Council on Nutrition, Metabolism, Obesity and cardiovascular disease: pathophysiology, evaluation, and effect of weight loss: an update of the 1997 American Heart Association Scientific Statement on Obesity and Heart Disease from the Obesity Committee of the Council on Nutrition, Physical Activity, and Metabolism, Circulation, 113 (2006) 898-918.

[2] Y. Zhang, J.R. Sowers, J. Ren, Targeting autophagy in obesity: from pathophysiology to management, Nat Rev Endocrinol, 14 (2018) 356-376.

[3] Y. Zhang, J. Ren, Epigenetics and obesity cardiomyopathy: From pathophysiology to prevention and management, Pharmacol Ther, 161 (2016) 52-66.

[4] E.D. Abel, S.E. Litwin, G. Sweeney, Cardiac remodeling in obesity, Physiol Rev, 88 (2008) 389-419.

[5] S. Wang, J. Ren, Obesity Paradox in Aging: From Prevalence to Pathophysiology, Prog Cardiovasc Dis, (2018).

[6] M.A. Alpert, K. Karthikeyan, O. Abdullah, R. Ghadban, Obesity and Cardiac Remodeling in Adults: Mechanisms and Clinical Implications, Prog Cardiovasc Dis, (2018).

[7] C.P. Cannon, Obesity-related cardiometabolic complications, Clin Cornerstone, 9 (2008) 11-19; discussion 20-12.

[8] I.J. Neeland, P. Poirier, J.P. Despres, Cardiovascular and Metabolic Heterogeneity of Obesity: Clinical Challenges and Implications for Management, Circulation, 137 (2018) 1391-1406.

ACCEPTED MANUSCRIPT

[9] M. Yanagisawa, H. Kurihara, S. Kimura, Y. Tomobe, M. Kobayashi, Y. Mitsui, Y. Yazaki, K. Goto, T. Masaki, A novel potent vasoconstrictor peptide produced by vascular endothelial cells, Nature, 332 (1988) 411-415.

[10] D. Prieto, C. Contreras, A. Sanchez, Endothelial dysfunction, obesity and insulin resistance, Curr Vasc Pharmacol, 12 (2014) 412-426.

[11] M. Cavalera, J. Wang, N.G. Frangogiannis, Obesity, metabolic dysfunction, and cardiac fibrosis: pathophysiological pathways, molecular mechanisms, and therapeutic opportunities, Transl Res, 164 (2014) 323-335.

[12] J. Fareh, R.M. Touyz, E.L. Schiffrin, G. Thibault, Endothelin-1 and angiotensin II receptors in cells from rat hypertrophied heart. Receptor regulation and intracellular Ca2+ modulation, Circ Res, 78 (1996) 302-311.

[13] K. Hasegawa, H. Fujiwara, M. Koshiji, T. Inada, S. Ohtani, K. Doyama, M. Tanaka, A. Matsumori, T. Fujiwara, G. Shirakami, K. Hosoda, K. Nakao, S. Sasayama, Endothelin-1 and its receptor in hypertrophic cardiomyopathy, Hypertension, 27 (1996) 259-264.

[14] B. Pieske, B. Beyermann, V. Breu, B.M. Loffler, K. Schlotthauer, L.S. Maier, S. Schmidt-Schweda, H. Just, G. Hasenfuss, Functional effects of endothelin and regulation of endothelin receptors in isolated human nonfailing and failing myocardium, Circulation, 99 (1999) 1802-1809.

[15] K. Asano, T.J. Bohlmeyer, J.Y. Westcott, L. Zisman, K. Kinugawa, M. Good, W.A. Minobe, R. Roden, E.E. Wolfel, J. Lindenfeld, J. David Port, M.B. Perryman, J. Clevel, B.D. Lowes, M.R. Bristow, Altered expression of endothelin receptors in failing human left ventricles, J Mol Cell Cardiol, 34 (2002) 833-846.

ACCEPTED MANUSCRIPT

[16] T. Kobayashi, T. Miyauchi, S. Sakai, M. Kobayashi, I. Yamaguchi, K. Goto, Y. Sugishita, Expression of endothelin-1, ETA and ETB receptors, and ECE and distribution of endothelin-1 in failing rat heart, Am J Physiol, 276 (1999) H1197-1206.

[17] S. Rich, V.V. McLaughlin, Endothelin receptor blockers in cardiovascular disease, Circulation, 108 (2003) 2184-2190.

[18] J. Bergler-Klein, R. Pacher, R. Berger, A. Bojic, B. Stanek, Neurohumoral and hemodynamic effects of the selective endothelin antagonist darusentan in advanced chronic heart failure, J Heart Lung Transplant, 23 (2004) 20-27.

[19] M. Barton, M. Yanagisawa, Endothelin: 20 years from discovery to therapy, Can J Physiol Pharmacol, 86 (2008) 485-498.

[20] A.F. Ceylan-Isik, M. Dong, Y. Zhang, F. Dong, S. Turdi, S. Nair, M. Yanagisawa, J. Ren, Cardiomyocyte-specific deletion of endothelin receptor A rescues aging-associated cardiac hypertrophy and contractile dysfunction: role of autophagy, Basic Res Cardiol, 108 (2013) 335.

[21] Y. Zhang, L. Li, Y. Hua, J.M. Nunn, F. Dong, M. Yanagisawa, J. Ren, Cardiac-specific knockout of ET(A) receptor mitigates low ambient temperature-induced cardiac hypertrophy and contractile dysfunction, J Mol Cell Biol, 4 (2012) 97-107.

[22] S.A. Nasser, M.M. El-Mas, Endothelin ETA receptor antagonism in cardiovascular disease, Eur J Pharmacol, 737 (2014) 210-213.

[23] R.M. Kedzierski, P.A. Grayburn, Y.Y. Kisanuki, C.S. Williams, R.E. Hammer, J.A. Richardson, M.D. Schneider, M. Yanagisawa, Cardiomyocyte-specific endothelin A receptor knockout mice have normal cardiac function and an unaltered hypertrophic response to angiotensin II and isoproterenol, Mol Cell Biol, 23 (2003) 8226-8232.

ACCEPTED MANUSCRIPT

[24] S. Wang, C. Wang, S. Turdi, K.L. Richmond, Y. Zhang, J. Ren, ALDH2 protects against high fat diet-induced obesity cardiomyopathy and defective autophagy: role of CaM kinase II, histone H3K9 methyltransferase SUV39H, Sirt1, and PGC-1alpha deacetylation, Int J Obes (Lond), 42 (2018) 1073-1087.

[25] A.F. Ceylan-Isik, N. Sreejayan, J. Ren, Endoplasmic reticulum chaperon tauroursodeoxycholic acid alleviates obesity-induced myocardial contractile dysfunction, J Mol Cell Cardiol, 50 (2011) 107-116.

[26] R. Guo, S. Nair, Y. Zhang, J. Ren, Adiponectin deficiency rescues high-fat diet-induced hepatic injury, apoptosis and autophagy loss despite persistent steatosis, Int J Obes (Lond), 41 (2017) 1403-1412.

[27] Y. Hua, T.J. Robinson, Y. Cao, G.P. Shi, J. Ren, S. Nair, Cathepsin K knockout alleviates aging-induced cardiac dysfunction, Aging Cell, 14 (2015) 345-351.

[28] F. Dong, X. Zhang, J. Ren, Leptin regulates cardiomyocyte contractile function through endothelin-1 receptor-NADPH oxidase pathway, Hypertension, 47 (2006) 222-229.

[29] S. Wang, X. Zhu, L. Xiong, Y. Zhang, J. Ren, Toll-like receptor 4 knockout alleviates paraquat-induced cardiomyocyte contractile dysfunction through an autophagy-dependent mechanism, Toxicol Lett, 257 (2016) 11-22.

[30] Z. Ye, G. Liu, J. Guo, Z. Su, Hypothalamic endoplasmic reticulum stress as a key mediator of obesity-induced leptin resistance, Obes Rev, 19 (2018) 770-785.

[31] C.X. Fang, T.A. Doser, X. Yang, N. Sreejayan, J. Ren, Metallothionein antagonizes aging-induced cardiac contractile dysfunction: role of PTP1B, insulin receptor tyrosine phosphorylation and Akt, Aging Cell, 5 (2006) 177-185.

ACCEPTED MANUSCRIPT

[32] A. Fukushima, G.D. Lopaschuk, Cardiac fatty acid oxidation in heart failure associated with obesity and diabetes, Biochim Biophys Acta, 1861 (2016) 1525-1534.

[33] A.K.S. Silva, C.A. Peixoto, Role of peroxisome proliferator-activated receptors in non-alcoholic fatty liver disease inflammation, Cell Mol Life Sci, 75 (2018) 2951-2961.

[34] C.D. Folmes, G.D. Lopaschuk, Role of malonyl-CoA in heart disease and the hypothalamic control of obesity, Cardiovasc Res, 73 (2007) 278-287.

[35] A.J. Lewis, S. Neubauer, D.J. Tyler, O.J. Rider, Pyruvate dehydrogenase as a therapeutic target for obesity cardiomyopathy, Expert Opin Ther Targets, 20 (2016) 755-766.

[36] S. Balasubramanian, R.K. Johnston, P.C. Moschella, S.K. Mani, W.J. Tuxworth, Jr., D. Kuppuswamy, mTOR in growth and protection of hypertrophying myocardium, Cardiovasc Hematol Agents Med Chem, 7 (2009) 52-63.

[37] S. Sakai, T. Miyauchi, T. Sakurai, Y. Kasuya, M. Ihara, I. Yamaguchi, K. Goto, Y. Sugishita, Endogenous endothelin-1 participates in the maintenance of cardiac function in rats with congestive heart failure. Marked increase in endothelin-1 production in the failing heart, Circulation, 93 (1996) 1214-1222.

[38] R. Yorikane, S. Sakai, T. Miyauchi, T. Sakurai, Y. Sugishita, K. Goto, Increased production of endothelin-1 in the hypertrophied rat heart due to pressure overload, FEBS Lett, 332 (1993) 31-34.

[39] P. Mulder, V. Richard, G. Derumeaux, M. Hogie, J.P. Henry, F. Lallemand, P. Compagnon, B. Mace, E. Comoy, B. Letac, C. Thuillez, Role of endogenous endothelin in chronic heart failure: effect of long-term treatment with an endothelin antagonist on survival, hemodynamics, and cardiac remodeling, Circulation, 96 (1997) 1976-1982.

ACCEPTED MANUSCRIPT

[40] H.M. Hong, E.J. Song, E. Oh, M.H. Kabir, C. Lee, Y.S. Yoo, Endothelin-1- and isoproterenol-induced differential protein expression and signaling pathway in HL-1 cardiomyocytes, Proteomics, 11 (2011) 283-297.

[41] J.R. Sowers, Obesity as a cardiovascular risk factor, Am J Med, 115 Suppl 8A (2003) 37S-41S.

[42] C.X. Fang, F. Dong, D.P. Thomas, H. Ma, L. He, J. Ren, Hypertrophic cardiomyopathy in high-fat diet-induced obesity: role of suppression of forkhead transcription factor and atrophy gene transcription, Am J Physiol Heart Circ Physiol, 295 (2008) H1206-H1215.

[43] H. Diedrichs, M. Chi, B. Boelck, U. Mehlhorn, R.H. Schwinger, Increased regulatory activity of the calcineurin/NFAT pathway in human heart failure, Eur J Heart Fail, 6 (2004) 3-9.

[44] H. Ehmke, J. Faulhaber, K. Munter, M. Kirchengast, R.J. Wiesner, Chronic ETA receptor blockade attenuates cardiac hypertrophy independently of blood pressure effects in renovascular hypertensive rats, Hypertension, 33 (1999) 954-960.

[45] T. Matsui, T. Nagoshi, A. Rosenzweig, Akt and PI 3-kinase signaling in cardiomyocyte hypertrophy and survival, Cell Cycle, 2 (2003) 220-223.

[46] S.E. Hardt, J. Sadoshima, Glycogen synthase kinase-3beta: a novel regulator of cardiac hypertrophy and development, Circ Res, 90 (2002) 1055-1063.

[47] I. Shiojima, M. Yefremashvili, Z. Luo, Y. Kureishi, A. Takahashi, J. Tao, A. Rosenzweig, C.R. Kahn, E.D. Abel, K. Walsh, Akt signaling mediates postnatal heart growth in response to insulin and nutritional status, J Biol Chem, 277 (2002) 37670-37677.

[48] A.H. Chaanine, R.J. Hajjar, AKT signalling in the failing heart, Eur J Heart Fail, 13 (2011) 825-829.

ACCEPTED MANUSCRIPT

[49] O.J. Kemi, M. Ceci, U. Wisloff, S. Grimaldi, P. Gallo, G.L. Smith, G. Condorelli, O. Ellingsen, Activation or inactivation of cardiac Akt/mTOR signaling diverges physiological from pathological hypertrophy, J Cell Physiol, 214 (2008) 316-321.

[50] J.R. McMullen, F. Amirahmadi, E.A. Woodcock, M. Schinke-Braun, R.D. Bouwman, K.A. Hewitt, J.P. Mollica, L. Zhang, Y. Zhang, T. Shioi, A. Buerger, S. Izumo, P.Y. Jay, G.L. Jennings, Protective effects of exercise and phosphoinositide 3-kinase(p110alpha) signaling in dilated and hypertrophic cardiomyopathy, Proc Natl Acad Sci U S A, 104 (2007) 612-617.

[51] J.R. McMullen, M.C. Sherwood, O. Tarnavski, L. Zhang, A.L. Dorfman, T. Shioi, S. Izumo, Inhibition of mTOR signaling with rapamycin regresses established cardiac hypertrophy induced by pressure overload, Circulation, 109 (2004) 3050-3055.

[52] L. Wang, I. Gout, C.G. Proud, Cross-talk between the ERK and p70 S6 kinase (S6K) signaling pathways. MEK-dependent activation of S6K2 in cardiomyocytes, J Biol Chem, 276 (2001) 32670-32677.

[53] D.D. Sarbassov, S.M. Ali, D.H. Kim, D.A. Guertin, R.R. Latek, H. Erdjument-Bromage, P. Tempst, D.M. Sabatini, Rictor, a novel binding partner of mTOR, defines a rapamycin-insensitive and raptor-independent pathway that regulates the cytoskeleton, Curr Biol, 14 (2004) 1296-1302.

[54] A.B. Gustafsson, R.A. Gottlieb, Recycle or die: the role of autophagy in cardioprotection, J Mol Cell Cardiol, 44 (2008) 654-661.

[55] N. Gurusamy, D.K. Das, Is autophagy a double-edged sword for the heart?, Acta Physiol Hung, 96 (2009) 267-276.

[56] S. Nair, J. Ren, Autophagy and cardiovascular aging: Lesson learned from rapamycin, Cell Cycle, 11 (2012).

ACCEPTED MANUSCRIPT

[57] J.A. Jacob, J.M.M. Salmani, Z. Jiang, L. Feng, J. Song, X. Jia, B. Chen, Autophagy: An overview and its roles in cancer and obesity, Clin Chim Acta, 468 (2017) 85-89.

[58] X. Xu, Y. Hua, S. Nair, Y. Zhang, J. Ren, Akt2 knockout preserves cardiac function in high-fat diet-induced obesity by rescuing cardiac autophagosome maturation, J Mol Cell Biol, 5 (2013) 61-63.

[59] L. Cao, X. Qin, M.R. Peterson, S.E. Haller, K.A. Wilson, N. Hu, X. Lin, S. Nair, J. Ren, G. He, CARD9 knockout ameliorates myocardial dysfunction associated with high fat diet-induced obesity, J Mol Cell Cardiol, 92 (2016) 185-195.

[60] C.H. Lai, C.C. Tsai, W.W. Kuo, T.J. Ho, C.H. Day, P.Y. Pai, L.C. Chung, C.C. Huang, H.F. Wang, P.H. Liao, C.Y. Huang, Multi-Strain Probiotics Inhibit Cardiac Myopathies and Autophagy to Prevent Heart Injury in High-Fat Diet-Fed Rats, Int J Med Sci, 13 (2016) 277-285.

[61] T. Schmelzle, M.N. Hall, TOR, a central controller of cell growth, Cell, 103 (2000) 253-262.

[62] C.J. Lavie, R.V. Milani, H.O. Ventura, Obesity and cardiovascular disease: risk factor, paradox, and impact of weight loss, J Am Coll Cardiol, 53 (2009) 1925-1932.

ACCEPTED MANUSCRIPT

ACCEPTED MANUSCRIPT

**Table 1.** List and sequence of primers used for RT-PCR.

| Gene | Forward | Reverse |
|---|---|---|
| ANP | 5’ – ACA GCC AAG GAG GAA AAG GC – 3’ | 5’ – CCA CAG TGG CAA TGT GAC CA – 3’ |
| BNP | 5’ – TCC AGA GCA ATT CAA GAT GCA – 3’ | 5’ – CTT TTG TGA GGC CTT GGT CC – 3’ |
| β-MHC | 5’ – GAT GTT TTT GTG CCC GAT GA – 3’ | 5’ – ACC GTC TTG CCA TTC TCC G – 3’ |
| GAPDH | 5’ – TGA AGC AGG CAT CTG AGG G – 3’ | 5’ – CGA AGG TGG AAG AGT GGG AG – 3’ |

ACCEPTED MANUSCRIPT

ACCEPTED MANUSCRIPT

**Table 2.** Biometric and echocardiographic properties in WT and $ET_AKO$ mice after 6 months of low- (10%) or high-fat (45%) diet intake.

| | WT-LF | WT-HF | ETAKO-LF | ETAKO-HF |
|---|---|---|---|---|
| Body Weight (g) | 21.4 ± 0.6 | 40.3 ± 5.5* | 21.7 ± 0.5 | 38.0 ± 1.0* |
| Heart Weight (mg) | 139 ± 3 | 212 ± 6* | 141 ± 4 | 153 ± 5# |
| HW/BW (mg/g) | 6.51 ± 0.12 | 5.27 ± 0.08 | 6.51 ± 0.21 | 4.06 ± 0.16 |
| Liver Weight (g) | 1.21 ± 0.03 | 1.41 ± 0.03* | 1.17 ± 0.03 | 1.35 ± 0.04* |
| LW/BW (mg/g) | 57.1 ± 2.2 | 35.2 ± 1.0* | 54.2 ± 1.69 | 35.6 ± 6.24* |
| Kidney Weight (g) | 0.320 ± 0.013 | 0.412 ± 0.015* | 0.341 ± 0.011 | 0.357 ± 0.010 |
| KW/BW (mg/kg) | 15.0 ± 0.5 | 10.3 ± 0.4* | 15.8 ± 0.7 | 9.5 ± 0.4* |
| LV EDD (mm) | 2.82 ± 0.05 | 3.25 ± 0.12* | 2.88 ± 0.16 | 3.11 ± 0.23 |
| LV ESD (mm) | 1.42 ± 0.01 | 2.14 ± 0.13* | 1.49 ± 0.06 | 1.65 ± 0.18# |
| Diastolic Wall Thickness (mm) | 1.00 ± 0.02 | 1.20 ± 0.01* | 1.04 ± 0.06 | 0.91 ± 0.03 |
| Heart Rate (beat per minute) | 515 ± 32 | 504 ± 39 | 505 ± 31 | 510 ± 26 |
| LV Mass (mg) | 64.7 ± 3.6 | 84.8 ± 1.9* | 67.4 ± 4.4 | 64.0 ± 6.6# |
| Fractional Shortening (%) | 52.1 ± 3.1 | 43.5 ± 2.6* | 48.1 ± 1.8 | 47.2 ± 2.6# |
| Ejection Fraction (%) | 87.3 ± 0.5 | 71.0 ± 3.7* | 85.8 ± 1.5 | 84.8 ± 2.4# |
| Diastolic BP (mmHg) | 76.3 ± 5.3 | 80.3 ± 4.3 | 74.8 ± 3.9 | 79.2 ± 4.5 |
| Systolic BP (mmHg) | 105.5 ± 6.7 | 119.7 ± 4.4* | 103.8 ± 3.1 | 121.5 ± 4.3* |
| Cardiac Triglycerides (μmol/g) | 4.38 ± 0.32 | 29.52 ± 3.10* | 2.44 ± 0.32 | 9.64 ± 1.80*# |

Mean ± SEM, n = 11-12 mice per group, *$p < 0.05$ *vs.* WT-LF group, #$p < 0.05$ vs. WT-HF group. HW: Heart weight; LW: Liver weight; KW: Kidney weight; LF: low fat; HF: high fat-diet; LV EDD: Left ventricular end diastolic diameter; LV ESD: Left ventricular end systolic diameter; BP: Blood pressure $ET_AKO$: Cardiac-specific $ET_A$ knockout.

ACCEPTED MANUSCRIPT

**Research highlights**

- We examined the effect of $ET_A$ receptor ablation on cardiac anomalies in diet-induced obesity;
- $ET_A$ knockout attenuated high fat diet-induced cardiac contractile anomalies;
- The effect of $ET_A$ ablation was related to restoration of autophagy;

ACCEPTED MANUSCRIPT

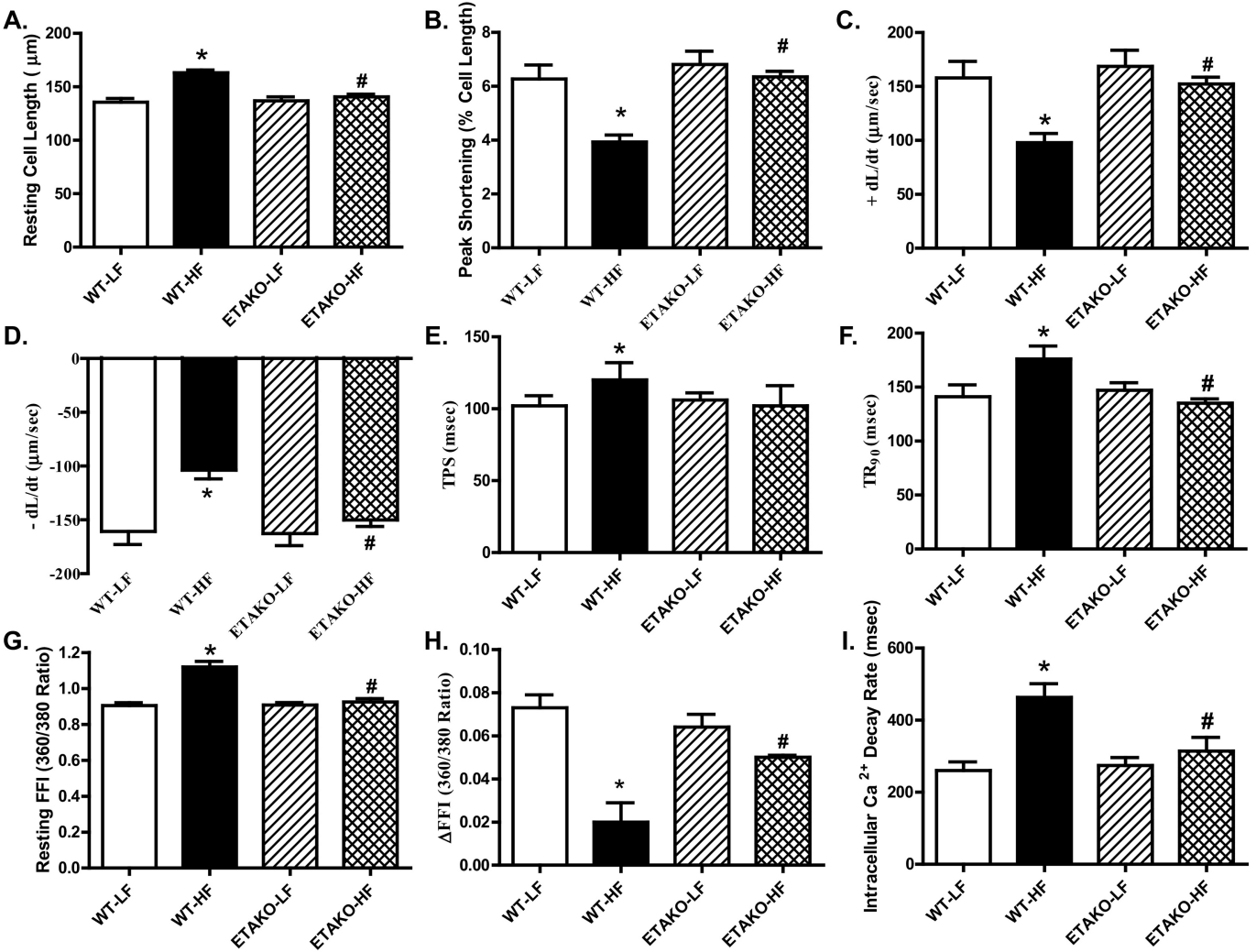

A.
Resting Cell Length ( μm)
200
150
100
50
0
*
#
WT-LF
WT-HF
ETAKO-LF
ETAKO-HF
B.
Peak Shortening (% Cell Length)
8
6
4
2
0
*
#
WT-LF
WT-HF
ETAKO-LF
ETAKO-HF
C.
+ dL/dt (μm/sec)
200
150
100
50
0
*
#
WT-LF
WT-HF
ETAKO-LF
ETAKO-HF
D.
- dL/dt (μm/sec)
0
-50
-100
-150
-200
*
#
WT-LF
WT-HF
ETAKO-LF
ETAKO-HF
E.
TPS (msec)
150
100
50
0
*
WT-LF
WT-HF
ETAKO-LF
ETAKO-HF
F.
TR90 (msec)
200
150
100
50
0
*
#
WT-LF
WT-HF
ETAKO-LF
ETAKO-HF
G.
Resting FFI (360/380 Ratio)
1.2
1.0
0.8
0.6
0.4
0.2
0.0
*
#
WT-LF
WT-HF
ETAKO-LF
ETAKO-HF
H.
ΔFFI (360/380 Ratio)
0.10
0.08
0.06
0.04
0.02
0.00
*
#
WT-LF
WT-HF
ETAKO-LF
ETAKO-HF
I.
Intracellular Ca 2+ Decay Rate (msec)
600
400
200
0
*
#
WT-LF
WT-HF
ETAKO-LF
ETAKO-HF

Figure 1

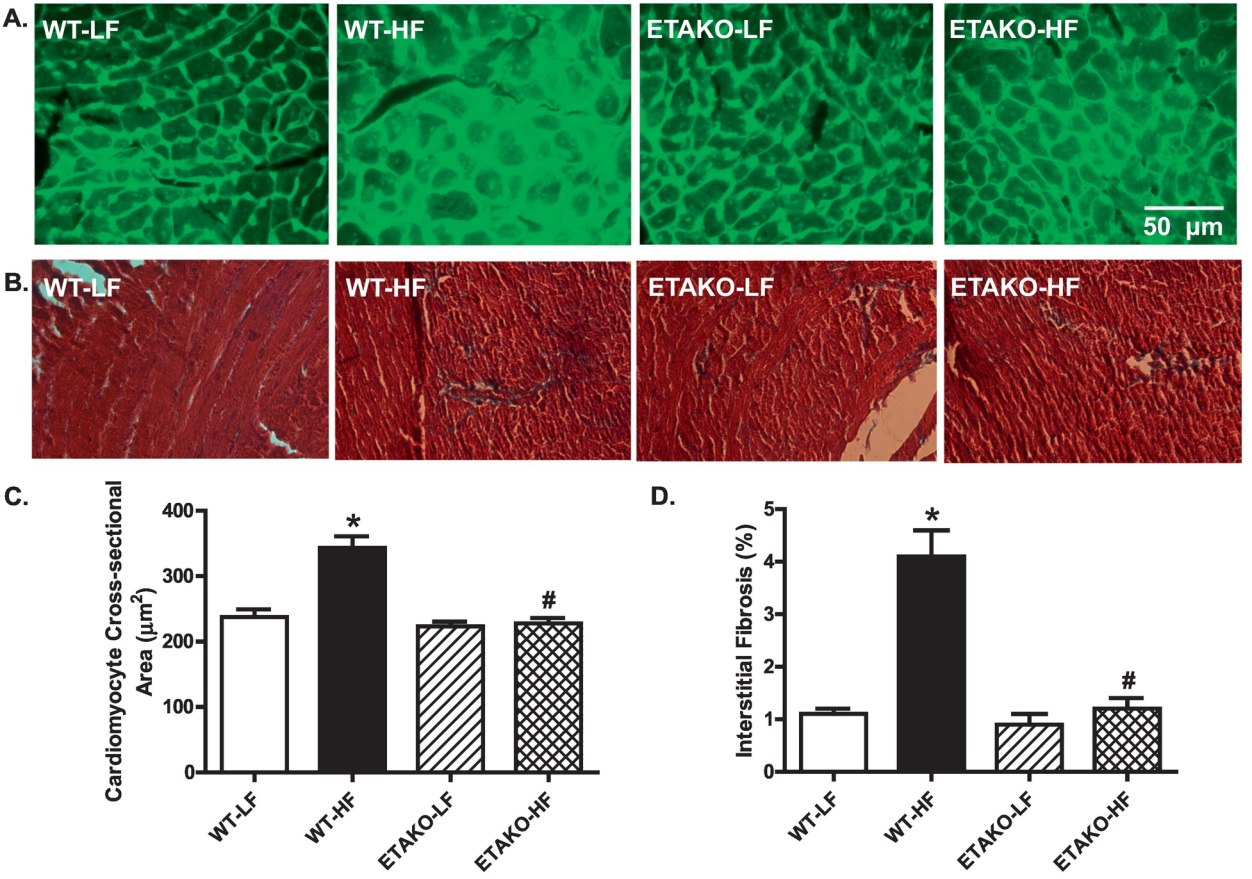
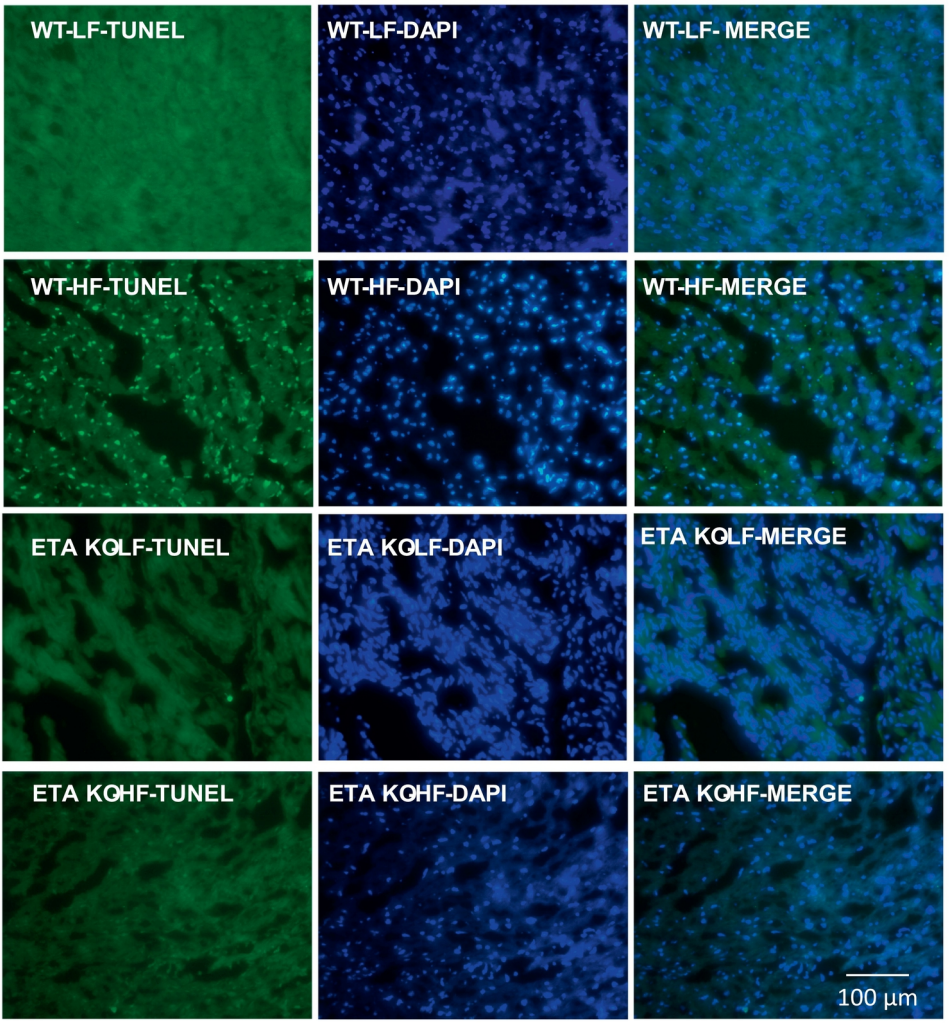

A.
WT-LF
WT-HF
ETAKO-LF
ETAKO-HF
50 μm
B.
WT-LF
WT-HF
ETAKO-LF
ETAKO-HF
C.
Cardiomyocyte Cross-sectional Area (μm²)
400
300
200
100
0
*
#
WT-LF
WT-HF
ETAKO-LF
ETAKO-HF
D.
Interstitial Fibrosis (%)
5
4
3
2
1
0
*
#
WT-LF
WT-HF
ETAKO-LF
ETAKO-HF

Figure 2


A.
WT-LF-TUNEL
WT-LF-DAPI
WT-LF- MERGE
WT-HF-TUNEL
WT-HF-DAPI
WT-HF-MERGE
ETA KOLF-TUNEL
ETA KOLF-DAPI
ETA KOLF-MERGE
ETA KOHF-TUNEL
ETA KOHF-DAPI
ETA KOHF-MERGE
100 µm

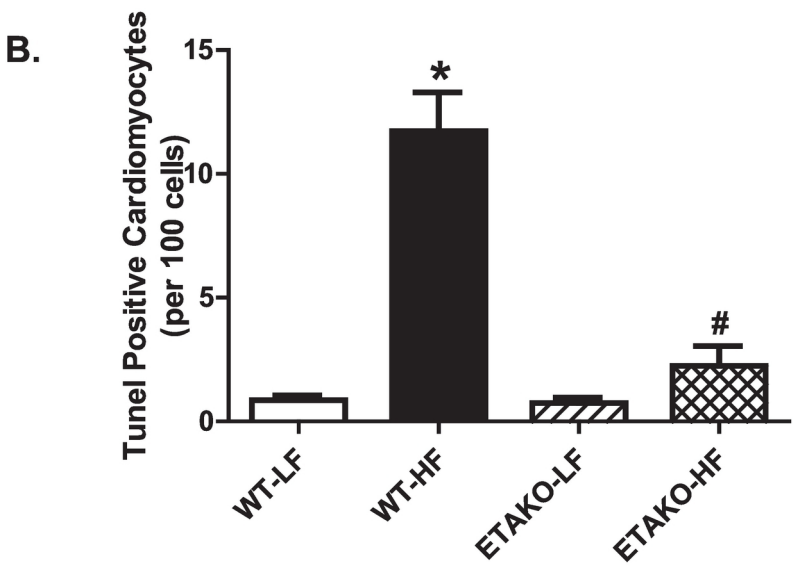

B.
Tunel Positive Cardiomyocytes (per 100 cells)
15
10
5
0
*
#
WT-LF
WT-HF
ETAKO-LF
ETAKO-HF

Figure 3

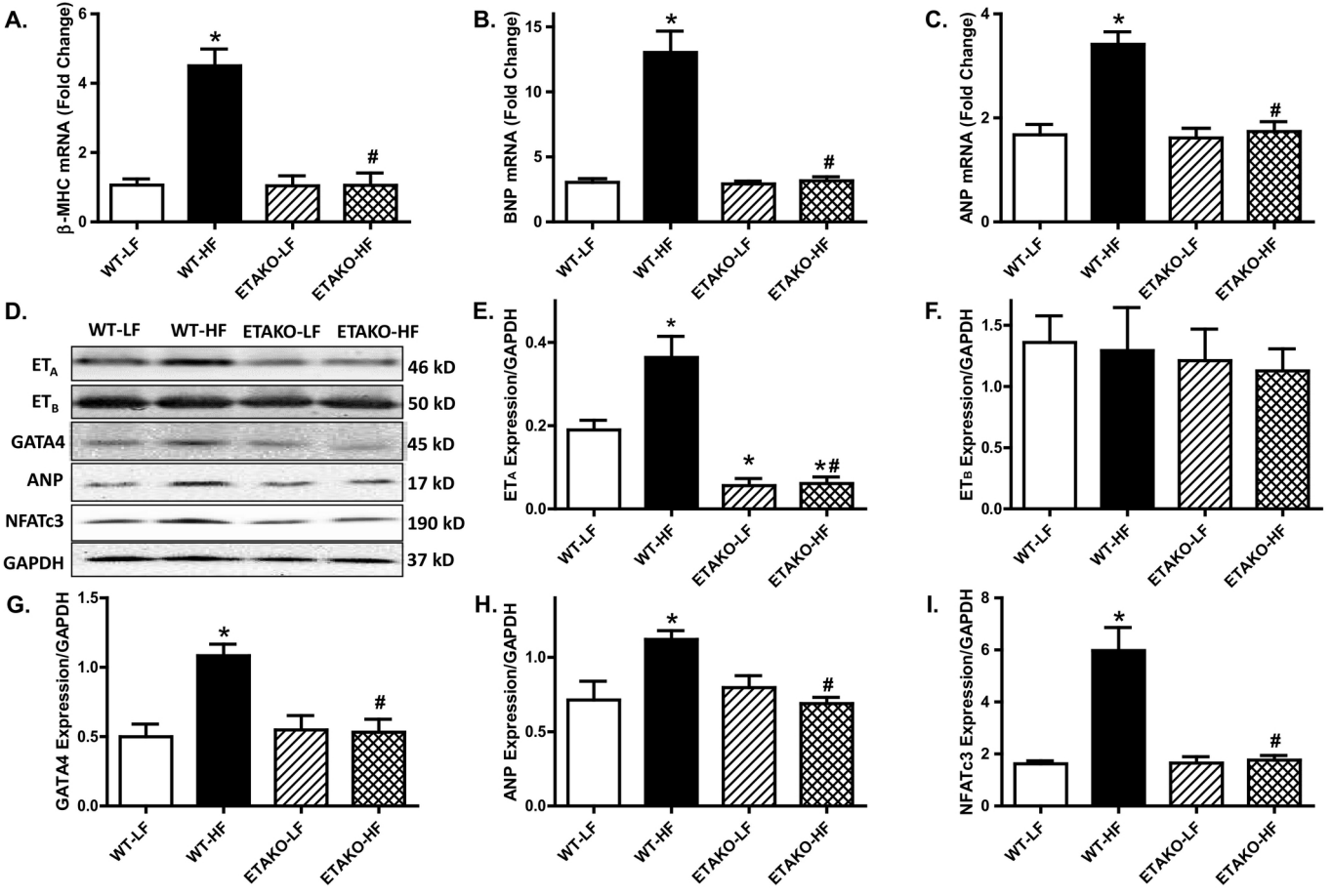

A.
β-MHC mRNA (Fold Change)
6
4
2
0
*
#
WT-LF
WT-HF
ETAKO-LF
ETAKO-HF
B.
BNP mRNA (Fold Change)
15
10
5
0
*
#
C.
ANP mRNA (Fold Change)
4
2
0
*
#
D.
WT-LF
WT-HF
ETAKO-LF
ETAKO-HF
ETA
46 kD
ETB
50 kD
GATA4
45 kD
ANP
17 kD
NFATc3
190 kD
GAPDH
37 kD
E.
ETA Expression/GAPDH
0.4
0.2
0.0
*
*#
F.
ETB Expression/GAPDH
1.5
1.0
0.5
0.0
G.
GATA4 Expression/GAPDH
1.5
1.0
0.5
0.0
*
#
H.
ANP Expression/GAPDH
1.0
0.5
0.0
*
#
I.
NFATc3 Expression/GAPDH
8
6
4
2
0
*
#

Figure 4

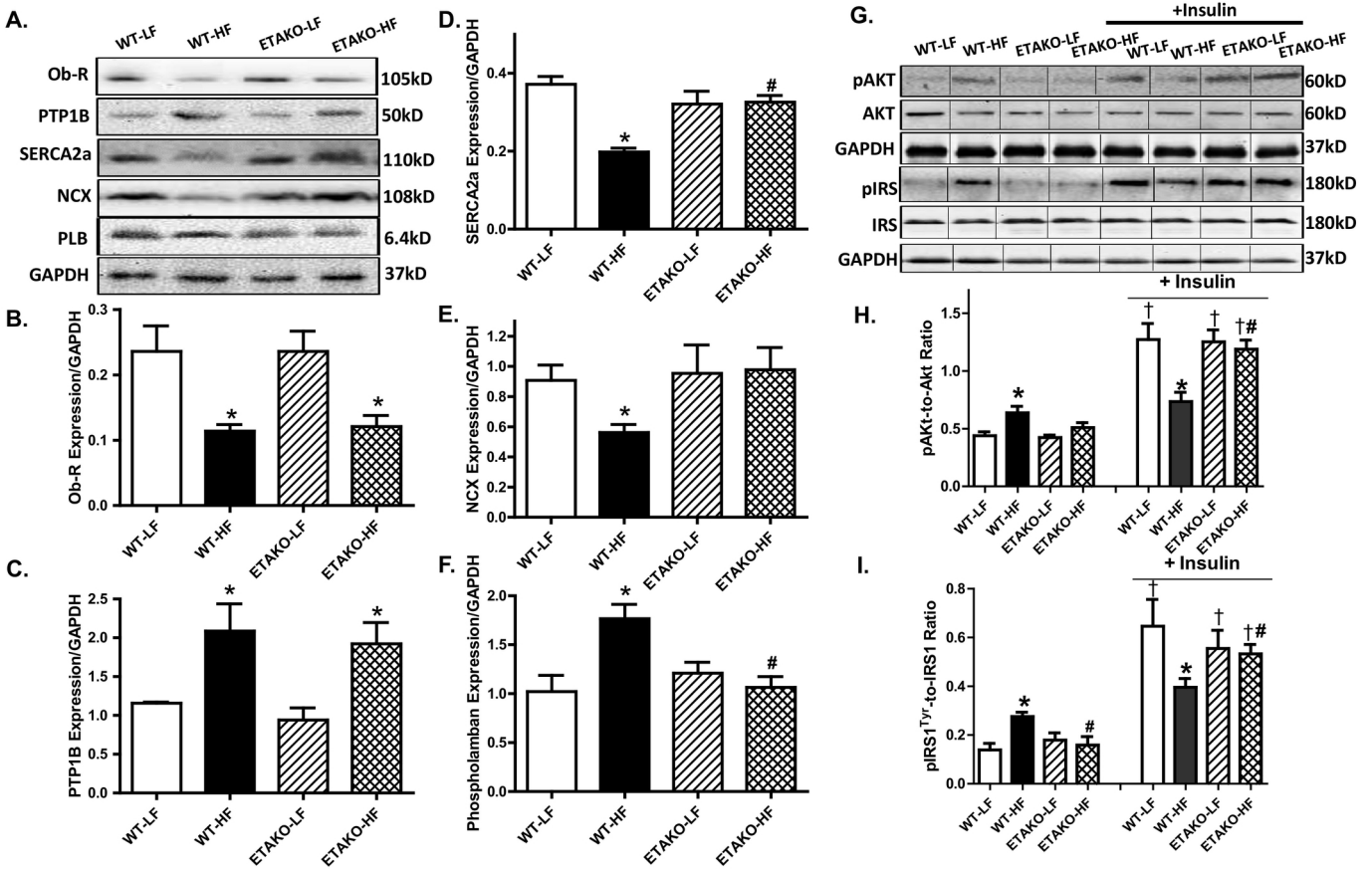

A.
WT-LF
WT-HF
ETAKO-LF
ETAKO-HF
Ob-R
105kD
PTP1B
50kD
SERCA2a
110kD
NCX
108kD
PLB
6.4kD
GAPDH
37kD
B.
Ob-R Expression/GAPDH
C.
PTP1B Expression/GAPDH
D.
SERCA2a Expression/GAPDH
E.
NCX Expression/GAPDH
F.
Phospholamban Expression/GAPDH
G.
+Insulin
pAKT
60kD
AKT
60kD
GAPDH
37kD
pIRS
180kD
IRS
180kD
GAPDH
37kD
H.
pAKt-to-Akt Ratio
+ Insulin
I.
pIRS1Tyr-to-IRS1 Ratio
+ Insulin

Figure 5

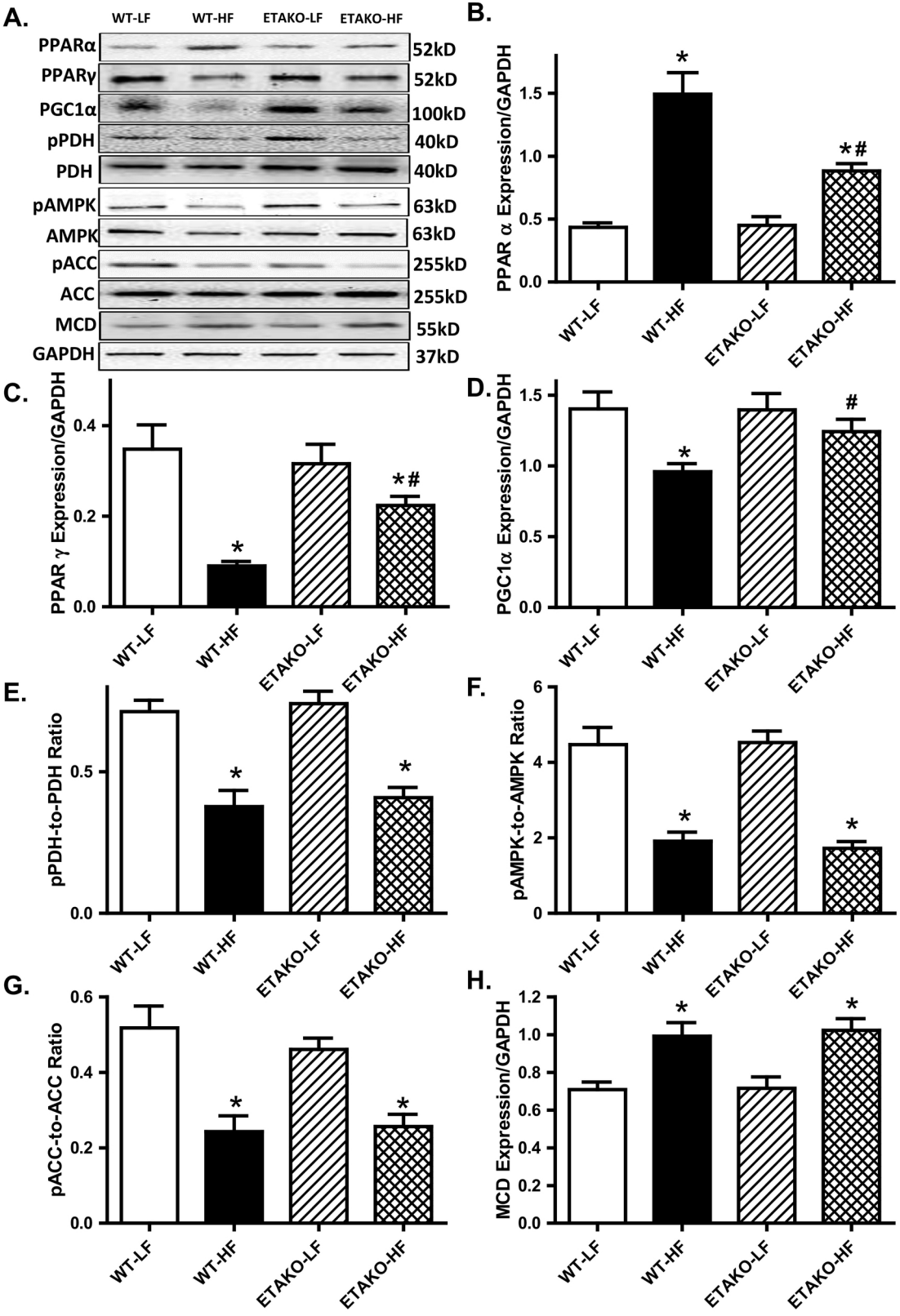

A.
WT-LF
WT-HF
ETAKO-LF
ETAKO-HF
PPARα
PPARγ
PGC1α
pPDH
PDH
pAMPK
AMPK
pACC
ACC
MCD
GAPDH
52kD
52kD
100kD
40kD
40kD
63kD
63kD
255kD
255kD
55kD
37kD
B.
PPAR α Expression/GAPDH
C.
PPAR γ Expression/GAPDH
D.
PGC1α Expression/GAPDH
E.
pPDH-to-PDH Ratio
F.
pAMPK-to-AMPK Ratio
G.
pACC-to-ACC Ratio
H.
MCD Expression/GAPDH

Figure 6

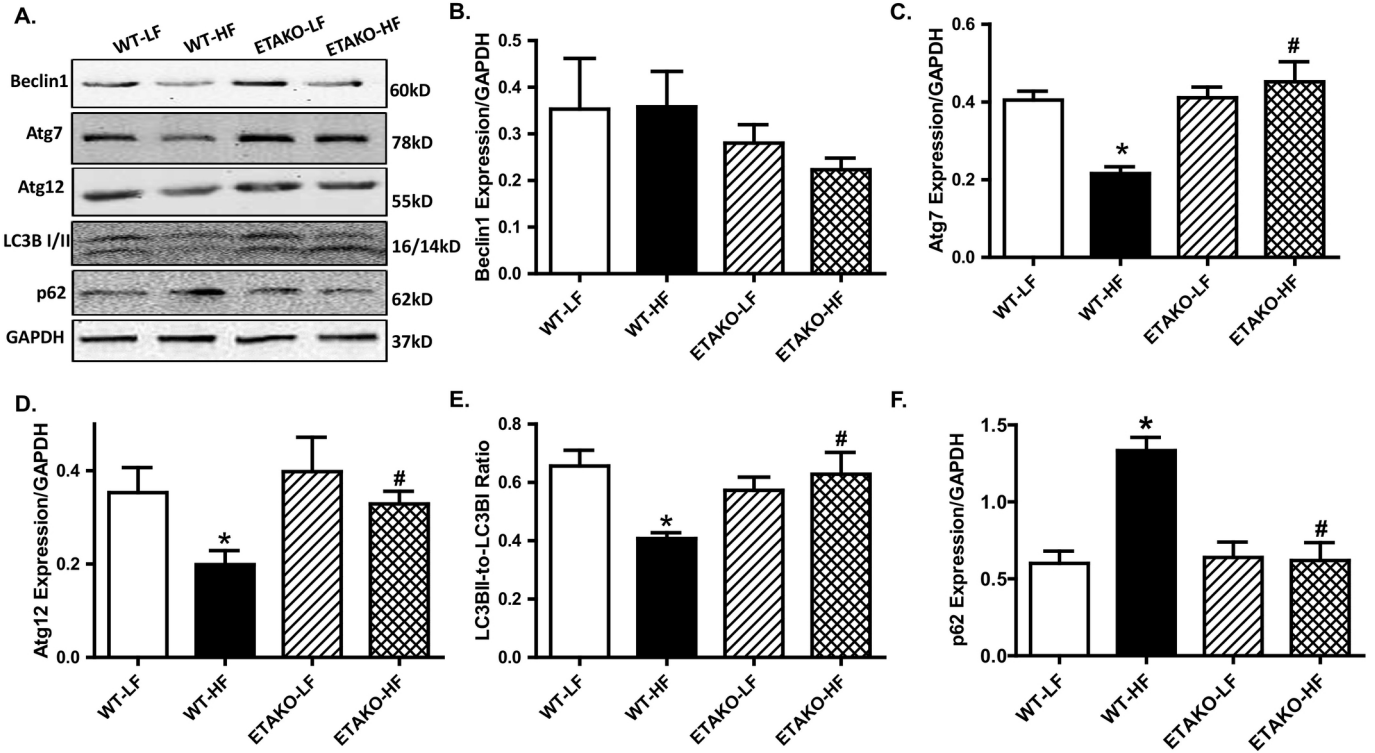

A.
WT-LF
WT-HF
ETAKO-LF
ETAKO-HF
Beclin1
Atg7
Atg12
LC3B I/II
p62
GAPDH
60kD
78kD
55kD
16/14kD
62kD
37kD
B.
Beclin1 Expression/GAPDH
C.
Atg7 Expression/GAPDH
D.
Atg12 Expression/GAPDH
E.
LC3BII-to-LC3BI Ratio
F.
p62 Expression/GAPDH

Figure 7

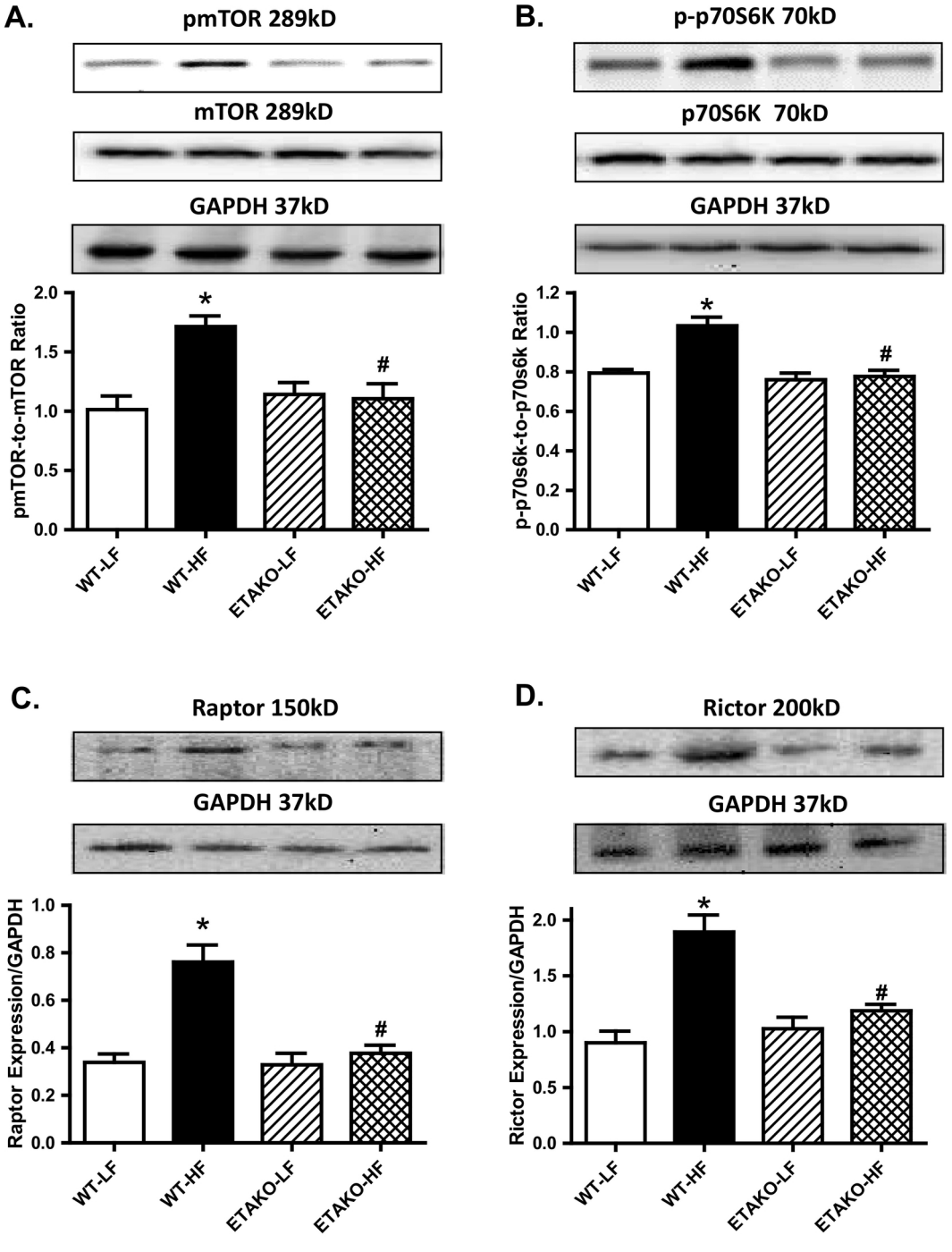

A.
pmTOR 289kD
mTOR 289kD
GAPDH 37kD
pmTOR-to-mTOR Ratio
2.0
1.5
1.0
0.5
0.0
*
#
WT-LF
WT-HF
ETAKO-LF
ETAKO-HF
B.
p-p70S6K 70kD
p70S6K 70kD
GAPDH 37kD
p-p70s6k-to-p70s6k Ratio
1.2
1.0
0.8
0.6
0.4
0.2
0.0
*
#
WT-LF
WT-HF
ETAKO-LF
ETAKO-HF
C.
Raptor 150kD
GAPDH 37kD
Raptor Expression/GAPDH
1.0
0.8
0.6
0.4
0.2
0.0
*
#
WT-LF
WT-HF
ETAKO-LF
ETAKO-HF
D.
Rictor 200kD
GAPDH 37kD
Rictor Expression/GAPDH
2.0
1.5
1.0
0.5
0.0
*
#
WT-LF
WT-HF
ETAKO-LF
ETAKO-HF

Figure 8

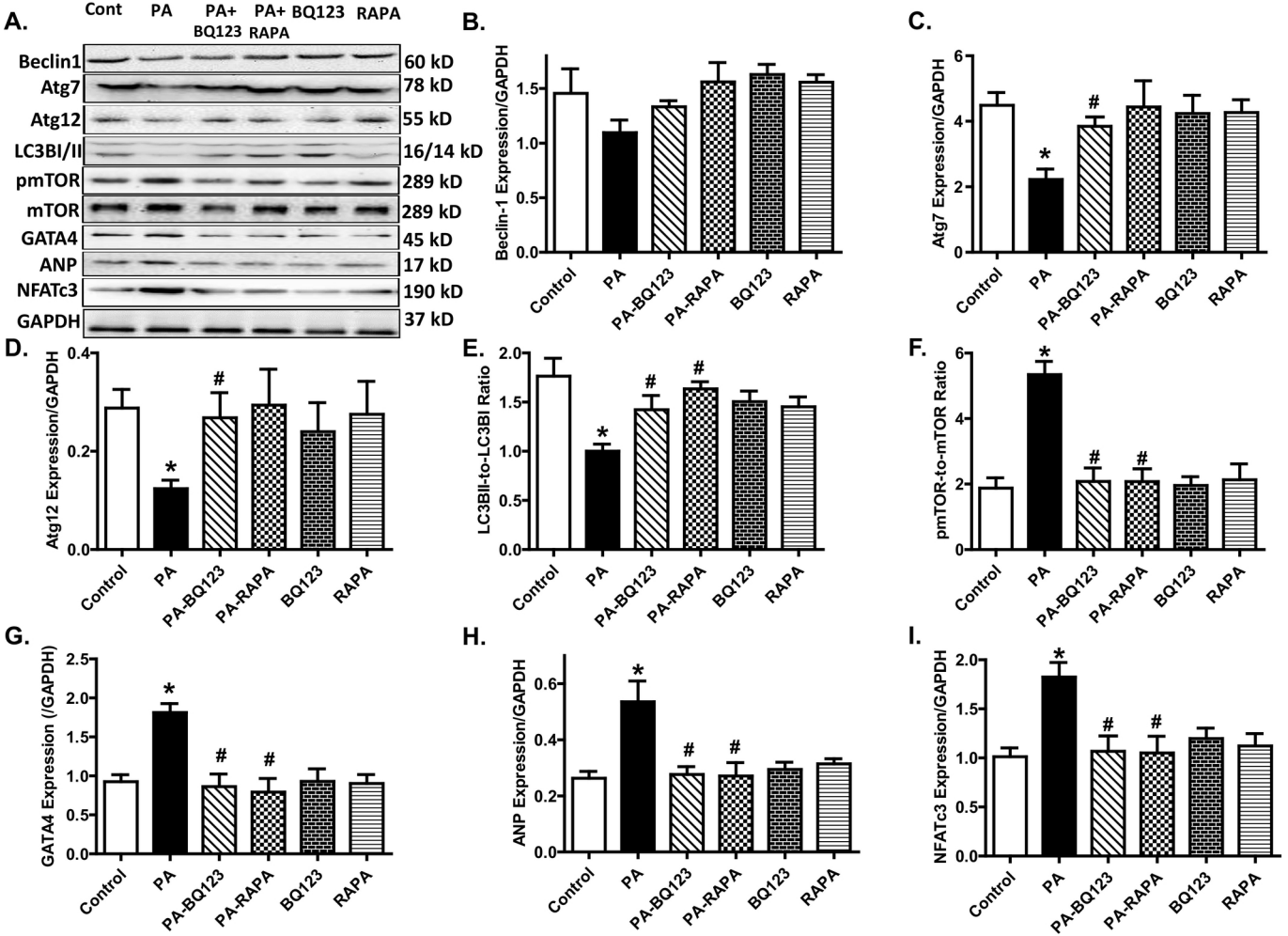

A.
Cont
PA
PA+ BQ123
PA+ RAPA
BQ123
RAPA
Beclin1
Atg7
Atg12
LC3BI/II
pmTOR
mTOR
GATA4
ANP
NFATc3
GAPDH
60 kD
78 kD
55 kD
16/14 kD
289 kD
289 kD
45 kD
17 kD
190 kD
37 kD
B.
Beclin-1 Expression/GAPDH
C.
Atg7 Expression/GAPDH
D.
Atg12 Expression/GAPDH
E.
LC3BII-to-LC3BI Ratio
F.
pmTOR-to-mTOR Ratio
G.
GATA4 Expression (/GAPDH)
H.
ANP Expression/GAPDH
I.
NFATc3 Expression/GAPDH
Control
PA
PA-BQ123
PA-RAPA
BQ123
RAPA

Figure 9

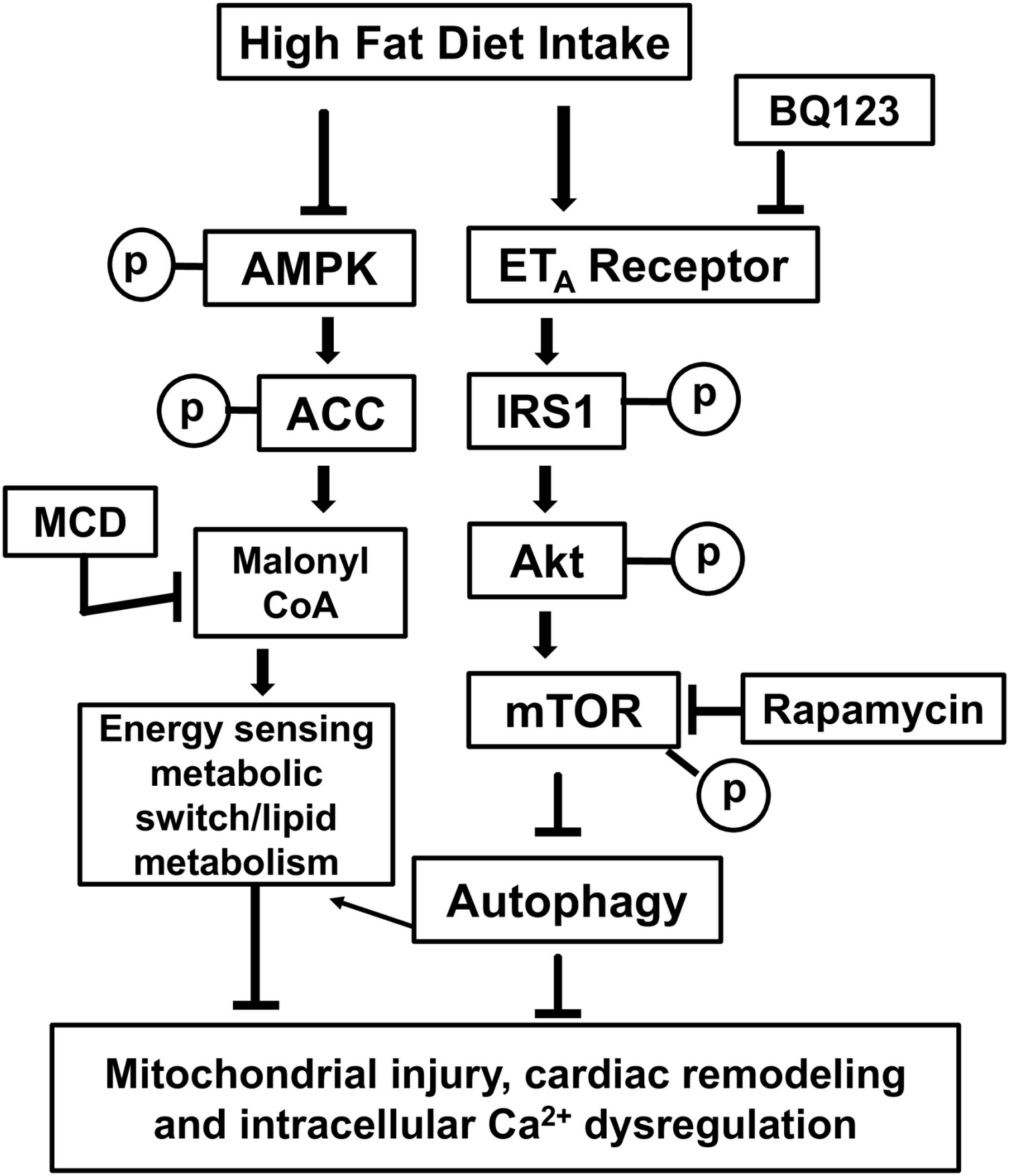

High Fat Diet Intake
BQ123
p
AMPK
ET$_A$ Receptor
p
ACC
IRS1
p
MCD
Malonyl CoA
Akt
p
mTOR
Rapamycin
p
Energy sensing metabolic switch/lipid metabolism
Autophagy
Mitochondrial injury, cardiac remodeling and intracellular $Ca^{2+}$ dysregulation

Figure 10